

FH535 inhibited metastasis and growth of pancreatic cancer cells

Meng-Yao Wu^{1,*}
 Rong-Rui Liang^{1,*}
 Kai Chen¹
 Meng Shen¹
 Ya-Li Tian^{1,2}
 Dao-Ming Li¹
 Wei-Ming Duan¹
 Qi Gui¹
 Fei-Ran Gong³
 Lian Lian^{1,2}
 Wei Li^{1,6}
 Min Tao^{1,4-6}

¹Department of Oncology, The First Affiliated Hospital of Soochow University, ²Department of Oncology, Suzhou Xiangcheng People's Hospital, ³Department of Hematology, The First Affiliated Hospital of Soochow University, ⁴Jiangsu Institute of Clinical Immunology, The First Affiliated Hospital of Soochow University, ⁵Institute of Medical Biotechnology, Soochow University, Suzhou, ⁶PREMED Key Laboratory for Precision Medicine, Soochow University, Suzhou, People's Republic of China

*These authors contributed equally to this work

Correspondence: Wei Li; Min Tao
 Department of Oncology, The First Affiliated Hospital of Soochow University, Suzhou 215006, People's Republic of China
 Tel +86 6778 0315; +86 6778 0310
 Fax +86 512 623 8798
 Email liwei10@suda.edu.cn;
 mtao@medmail.com.cn

Abstract: FH535 is a small-molecule inhibitor of the Wnt/ β -catenin signaling pathway, which a substantial body of evidence has proven is activated in various cancers, including pancreatic cancer. Activation of the Wnt/ β -catenin pathway plays an important role in tumor progression and metastasis. We investigated the inhibitory effect of FH535 on the metastasis and growth of pancreatic cancer cells. Western blotting and luciferase reporter gene assay indicated that FH535 markedly inhibited Wnt/ β -catenin pathway viability in pancreatic cancer cells. In vitro wound healing, invasion, and adhesion assays revealed that FH535 significantly inhibited pancreatic cancer cell metastasis. We also observed the inhibitory effect of FH535 on pancreatic cancer cell growth via the tetrazolium and plate clone formation assays. Microarray analyses suggested that changes in the expression of multiple genes could be involved in the anti-cancer effect of FH535 on pancreatic cancer cells. Our results indicate for the first time that FH535 inhibits pancreatic cancer cell metastasis and growth, providing new insight into therapy of pancreatic cancer.

Keywords: pancreatic cancer, FH535, β -catenin, metastasis, growth

Introduction

Pancreatic cancer is one of the most aggressive human malignancies worldwide. Despite improvements in surgical and chemotherapeutic approaches over the past decades, the prognosis of pancreatic cancer remains dismal; the average overall 5-year survival rate is <5%.¹ The reasons for this are the challenges associated with diagnosis, which tends to be late and uncertain; more importantly, therapeutic options are limited. Even with early diagnosis and surgical resection with curative intention, nearly all patients develop local recurrence or distant metastases following surgery and eventually succumb to the debilitating effects of metastatic growth.^{2,3} Conventional chemotherapy is rarely curative for metastatic pancreatic cancer. In recent years, there have been important advances in the organization of care for patients with pancreatic cancer; these advances have also resulted in more focused studies on surgical, oncological, and immunological treatment.

The Wnt/ β -catenin pathway is a genetically conserved signaling pathway associated with a variety of human conditions such as birth defects and tumors. Abnormal Wnt/ β -catenin pathway activation is closely related to the development of many cancers.^{4,5} An increasing amount of evidence demonstrates that both the β -catenin-dependent (canonical) and β -catenin-independent (non-canonical) Wnt signaling pathways play a key role in regulating pathological processes by facilitating tumor growth, migration, and invasion. In canonical Wnt signaling, glycogen synthase kinase-3 β (GSK-3 β) phosphorylates β -catenin at certain key residues, leading to its ubiquitination and subsequent degradation.^{5,6} Non-phosphorylated β -catenin accumulates in the cytoplasm,

and pathway activation leads to nuclear accumulation of β -catenin and interaction with T-cell factor (TCF) transcription factors, subsequently stimulating the downstream target genes, which include the genes participating in cell metastasis and proliferation.^{7,8}

Abnormal Wnt/ β -catenin pathway activation plays an important role in human pancreatic cancer, where it causes extracellular matrix degradation and uncontrolled cell proliferation and differentiation.⁹ Recent studies have demonstrated that FH535 is a synthetic inhibitor of the canonical Wnt signaling pathway; it inhibits the growth of colon, lung, breast, and hepatocellular carcinoma lines,^{10,11} suggesting that small-molecule targeting of the Wnt/ β -catenin pathway could be a promising therapeutic approach for cancers in which this pathway is activated.

In this study, we investigated the anti-cancer effect of FH535 on pancreatic cancer and explored the mechanisms underlying the effect, providing a rationale for further development of FH535 as a promising therapeutic agent for treating pancreatic cancer.

Materials and methods

Cell cultures and reagents

The human pancreatic cancer cell lines PANC-1 and BxPC-3 were purchased from American Type Culture Collection (ATCC) (Manassas, VA, USA). The cells were maintained in Dulbecco's Modified Eagle's Medium (DMEM; Thermo Fisher Scientific, Waltham, MA, USA) supplemented with 10% fetal calf serum (FCS), 100 U/mL penicillin, and 100 μ g/mL streptomycin (Thermo Fisher Scientific) at 37°C in a 5% CO₂ incubator under a humidified atmosphere; the cells were passaged every 2–3 days for exponential growth. FH535 was purchased from EMD Millipore (Billerica, MA, USA).

Western blotting

Total protein was extracted using a lysis buffer (50 mM Tris-HCl [pH 7.4], 150 mM NaCl, 1% Triton X-100, 0.1% sodium dodecyl sulfate [SDS], 1 mM EDTA) supplemented with a protease inhibitor cocktail kit and a phosphatase inhibitor cocktail kit (Hoffman-La Roche Ltd., Basel, Switzerland). The protein extracts were loaded, size-fractionated by SDS-polyacrylamide gel electrophoresis, and transferred to polyvinylidene difluoride membranes (Bio-Rad Laboratories Inc., Hercules, CA, USA). After blocking, the membranes were incubated with the primary antibodies mouse anti- β -catenin (Santa Cruz Biotechnology Inc., Dallas, TX, USA) and rabbit anti- β -actin (Proteintech Group Inc., Chicago, IL, USA) at 4°C overnight. Protein expression was determined using horseradish peroxidase-conjugated anti-mouse or anti-rabbit secondary antibodies, followed by detection using enhanced

chemiluminescence (EMD Millipore). Band intensity was visualized using a JS-1035 image analysis scanning system (Shanghai Peiqing Science & Technology, Co., Ltd., Shanghai, People's Republic of China).

Luciferase reporter assay

β -catenin is a dominant factor in the Wnt/ β -catenin/TCF signaling pathway, which regulates gene transcription by binding β -catenin and TCF. The activity of this final step in the pathway can be precisely measured using a luciferase reporter construct. The reporter plasmid pTOPFLASH (TCF reporter plasmid; EMD Millipore) contains two sets (the second set is in the reverse orientation) of three copies of the TCF binding site (wild-type) upstream of the thymidine kinase minimal promoter and luciferase open reading frame. The internal control plasmid pRL-SV40 (Promega Corporation, Fitchburg, WI, USA) contains the *Renilla* luciferase gene. Cells were transiently cotransfected with pTOPFLASH plasmid (500 ng/well) and pRL-SV40 plasmid (100 ng/well) for 6 hours using Lipofectamine 2000 (Thermo Fisher Scientific) according to the manufacturer's protocol. Then, the medium was renewed and FH535 was added. After 24 hours of treatment, cell lysates were subjected to the dual luciferase reporter assay according to the manufacturer's recommendations; luciferase activity was measured using a luminometer (Turner Designs, Sunnyvale, CA, USA). The results are expressed as relative luciferase activity, ie, the ratio of firefly luciferase activity over *Renilla* luciferase activity.

Wound healing assay

Cells (1×10^4 /well) were seeded in 96-well plates and grown to confluence. The monolayer culture was artificially scrape wounded with a sterile micropipette tip to create a denuded zone of constant width. Each well was washed with phosphate-buffered saline twice to remove the detached cells before FH535 treatment. Cell migration to the wounded region was observed using an XDS-1B inverted microscope (MIC Optical and Electrical Instrument, Chongqing, People's Republic of China) and photographed ($\times 40$ magnification). Images were captured at 0, 8, and 12 hours to monitor the wound healing process. The wound areas were measured using ImageJ (NIH, Bethesda, MA, USA).

Transwell invasion assay

We used a 24-well Transwell plate with an 8 μ m pore size polycarbonate filter membrane (Corning Incorporated, Corning, NY, USA). Cells (1×10^5) in 100 μ L serum-free DMEM were added to the Matrigel-coated top chamber (BD Biosciences, San Jose, CA, USA); the bottom chamber contained

DMEM with 10% FCS. The cells were incubated for 24 hours; cells that had invaded through the Matrigel-coated membrane were fixed and stained with crystal violet and counted under a light microscope in five random fields in a blinded fashion.

Adhesion assay

Cells were resuspended in complete medium and seeded in 24-well plates at 1×10^4 cells/mL. After 5-hour incubation, the unattached cells were removed to another well. The attached and unattached cells were evaluated using the 3-[4,5-dimethylthiazol-2-yl] 2,5-diphenyltetrazolium bromide (MTT) assay. The adhesion rate was calculated as follows: (absorbance of attached cells/[absorbance of attached cells + absorbance of unattached cells]) $\times 100\%$.

MTT assay

Cell growth was evaluated using the MTT assay. Cells (5×10^4 /well) were seeded in 24-well tissue culture plates. Blank control was treated with DMSO. After FH535 treatment, MTT (Sigma-Aldrich Co., St Louis, MO, USA) was added to each well (final concentration, 0.5 mg/mL), followed by 4-hour incubation at 37°C. The medium was removed, and 800 μ L of dimethyl sulfoxide was added to each well. The absorbance of the mixture was measured at 490 nm using a microplate enzyme-linked immunosorbent assay reader (Bio-Rad Laboratories Inc.). The relative cell viability was calculated as follows: relative cell viability = (mean experimental absorbance/mean control absorbance) $\times 100\%$.

Plate clone formation assay

Cells (200/well) were seeded in 24-well plates and treated after 12 hours. After 15 days, the cells were stained with 1% methylrosanilinium chloride, and the number of visible colonies was counted. The relative clone formation ability was calculated as follows: (mean experimental clone number/mean control clone number) $\times 100\%$.

Cell cycle analysis

Before treatment, the cells were serum starved for 24 hours to synchronize the cell cycle. Then, FCS was added to the cells, followed by various concentrations of FH535. Following 24 hours of FH535 treatment, the cells were fixed in 80% cooled ethanol and incubated with 0.5% Triton X-100 solution containing 1 mg/mL RNase A at 37°C for 30 minutes. Next, propidium iodide (Sigma-Aldrich Co.) was added to the wells (final concentration, 50 μ g/mL), followed by 30-minute incubation in the dark. Cellular DNA content was analyzed using a fluorescence-activated cell sorter (Becton Dickinson, Franklin Lakes, NJ, USA). Data

were processed using ModFit LT software (Verity Software House, Topsham, ME, USA).

Microarray assay

Sample preparation and processing were performed as described in the GeneChip Expression Analysis Manual (Agilent Technologies, Santa Clara, CA, USA). Differentially expressed genes were screened using Agilent 44K human whole-genome oligonucleotide microarrays. The selection criterion was greater than twofold difference in expression (difference in upregulated expression was greater than twofold; difference in downregulated expression was less than 0.5-fold). Hierarchical clustering of samples was performed using an average linkage algorithm using TIGR MultiExperiment Viewer (The Institute for Genomic Research, Rockville, MD, USA).

Statistical analysis

Each experiment was performed in at least triplicate. Results are expressed as the mean \pm standard deviation. Statistical analysis was performed using an unpaired Student's *t*-test. $P < 0.05$ was considered significant.

Results

FH535 inhibited the β -catenin pathway in pancreatic cancer cells

Treatment with 20 μ M FH535¹² did not affect nuclear or total β -catenin expression in the BxPC-3 cells, but downregulated nuclear and total β -catenin in the PANC-1 cells (Figure 1A). The luciferase reporter assay confirmed that FH535 suppressed TCF-dependent transcription, which may have led to dysregulation of the genes downstream of the β -catenin pathway (Figure 1B). To verify this, we performed microarray analyses to determine the mRNA expression changes in 138 genes downstream of the β -catenin pathway using Agilent 44K human whole-genome oligonucleotide microarrays (http://www.stanford.edu/group/nusselab/cgi-bin/wnt/target_genes); 20 μ M FH535 upregulated or downregulated multiple genes (Figure 1C, Table 1).

FH535 inhibited pancreatic cancer cell migration

In all, 20 μ M FH535 inhibited pancreatic cancer cell migration in a time-dependent manner (Figure 2A). To investigate the mechanisms involved, we analyzed the microarray data to illustrate the expression of genes participating in focal adhesion (Figure 2B, Table 2),^{13,14} adhesion junctions (Figure 2C, Table 3),^{15–17} tight junctions (Figure 2D, Table 4),^{18–23} and cell motility (Figure 2E, Table 5).^{24–27}

FH535 inhibited pancreatic cancer cell invasion

The Matrigel invasion assay revealed that FH535-treated cells had significantly decreased invasive capacity as compared with the control cells (Figure 3A), supporting the premise that FH535 inhibits pancreatic cancer cell invasion. Moreover, FH535 inhibited the adhesion ability of pancreatic cancer cells dose-dependently (Figure 3C). We also analyzed the microarray data to explore the changes in the expression of genes involved in the *in vitro* invasion process, including extracellular matrix degradation (Figure 3B, Table 6), cell adhesion (Figure 3D, Table 7),^{28,29} and epithelial–mesenchymal transition (EMT) (Figure 3E, Table 8).^{30–33}

FH535 inhibited pancreatic cancer cell growth

Using MTT assay, we evaluated the inhibitory effect of FH535 on pancreatic cancer cell line growth. The proliferation of PANC-1 and BxPC-3 cells cultured for up to 48 hours with FH535 was significantly inhibited time-dependently and dose-dependently as compared to the control cells (Figure 4A). The clone formation assays confirmed the dose-dependent

inhibitory effect of FH535 on pancreatic cancer cell growth (Figure 4B). We performed cell cycle analysis to confirm the antimetogenic effect of FH535. FH535 induced G2/M accumulation and decreased the cell population in the G0/G1 and S phases dose-dependently (Figure 4C). The expression profile of the cell cycle–related genes obtained from microarray analyses was analyzed (Figure 4D, Table 9).³⁴

Discussion

It is widely acknowledged that the prognosis of pancreatic cancer is very poor. The canonical Wnt/ β -catenin signaling pathway plays a key role in tumor development and dissemination. Classical Wnt signaling pathway causes accumulation of β -catenin in cytoplasm in complex with the transcription factor TCF/LEF that regulates target gene expression.^{9,35} Dysregulation of Wnt/ β -catenin signaling and altered transcription of β -catenin/TCF-regulated genes are found in many cancers,³⁶ including pancreatic cancer.³⁷ In this regard, we focused on characterizing the mechanisms of the anti-tumor effect of FH535 on pancreatic cancer cells.

Western blotting revealed that FH535 did not affect β -catenin expression in BxPC-3 cells. Interestingly, FH535

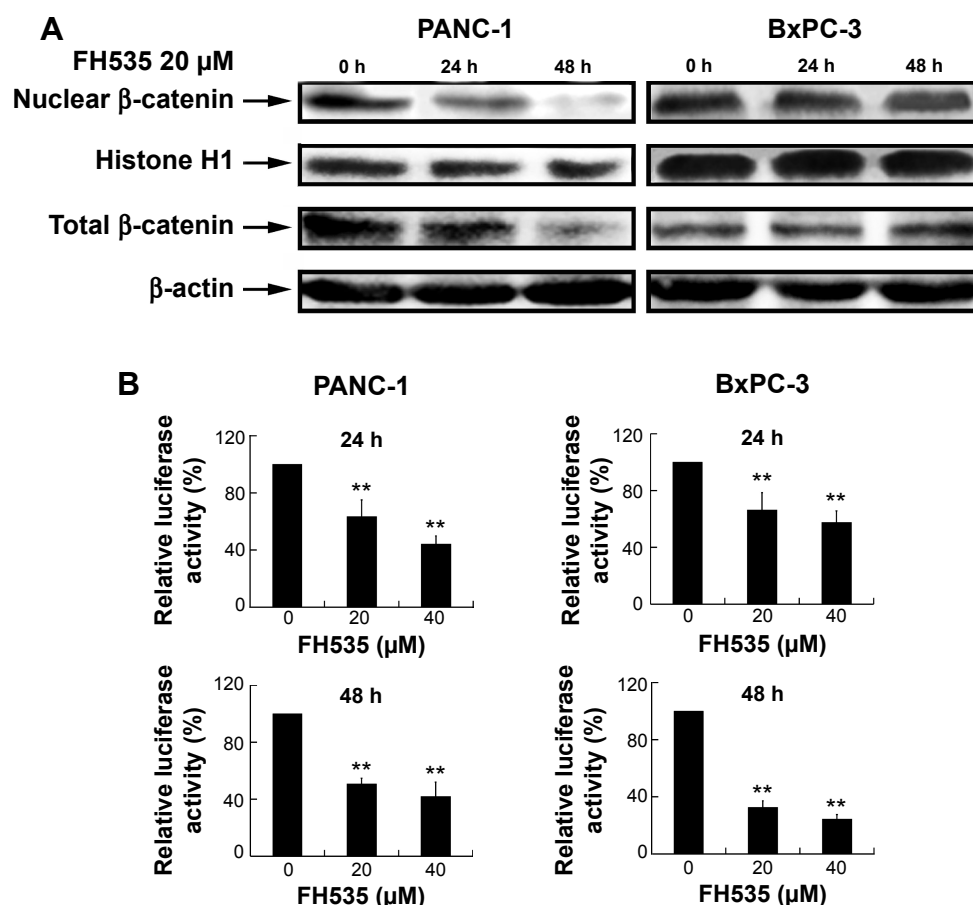


Figure 1 (Continued)

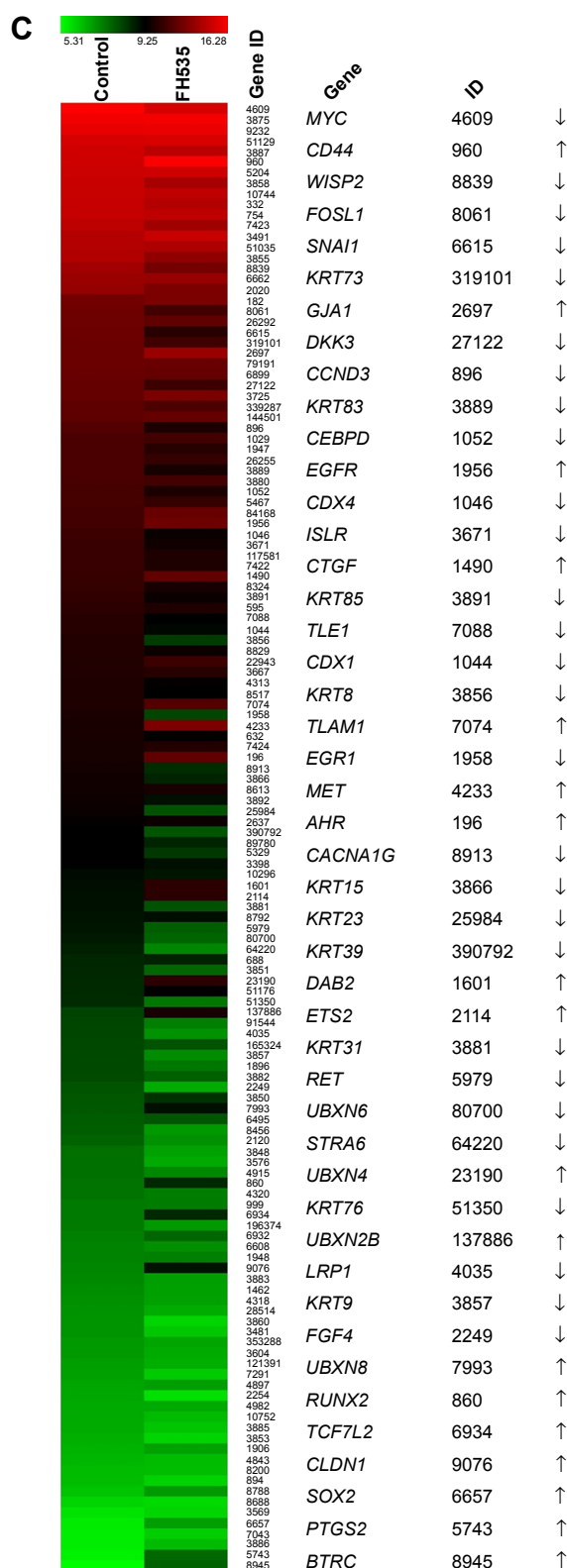


Figure 1 FH535 suppressed the Wnt/β-catenin pathway in pancreatic cancer cells.

Notes: (A) Time-dependent decrease by FH535 of nuclear and total β-catenin protein levels in PANC-1 cells; FH535 did not affect nuclear or total β-catenin expression in BxPC-3 cells. (B) Dose-dependent decrease by FH535 of TCF-dependent transcription. $^{***}P < 0.01$, significant differences vs the respective control groups. (C) Microarray analysis of expression regulation of genes downstream of the Wnt/β-catenin pathway upon 20 μM FH535 treatment. Up and down arrows indicate gene expression significantly upregulated or downregulated, respectively, by twofold. **Abbreviations:** TCF, T-cell factor; h, hours.

Table 1 Microarray analysis of expression regulation of genes downstream of the Wnt/β-catenin pathway upon 20 μM FH535 treatment

Gene	ID	Normalized intensity	
		Control	FH535
MYC	4609	16.268158	15.204586
KRT18	3875	15.975001	16.022995
PTTG1	9232	15.680945	15.73604
ANGPTL4	51129	15.190848	15.278334
KRT81	3887	15.0413	14.423697
CD44	960	15.006962	16.199093
PFDN5	5204	14.879261	14.964103
KRT10	3858	14.799751	13.889791
PTTG2	10744	14.772796	14.547727
BIRC5	332	14.757564	14.219355
PTTG1IP	754	14.684395	14.533192
VEGFB	7423	14.498004	13.671163
CYR61	3491	14.279853	14.790296
UBXN1	51035	14.231482	14.049252
KRT7	3855	14.184294	13.285099
WISP2	8839	13.732449	12.493675
SOX9	6662	13.574989	13.415171
EN2	2020	13.393019	12.721889
JAG1	182	12.427784	12.687155
FOSL1	8061	12.344017	11.102832
MYCBP	26292	12.284651	11.974781
SNAI1	6615	12.28132	10.385736
KRT73	319101	12.23975	11.053284
GJA1	2697	12.226766	13.521647
IRX3	79191	12.224495	12.16053
TBX1	6899	12.181493	12.043698
DKK3	27122	12.076692	10.961267
JUN	3725	12.038464	12.673436
MSL1	339287	11.920114	11.438548
KRT80	144501	11.87818	12.039767
CCND3	896	11.576098	10.075832
CDKN2A	1029	11.343829	11.097562
EFNB1	1947	11.337793	10.368351
PTTG3P	26255	11.33311	10.750982
KRT83	3889	11.319811	9.89329
KRT19	3880	11.289505	11.101922
CEBPD	1052	11.196305	10.068165
PPARD	5467	11.19087	10.731722
ANTXR1	84168	11.149265	12.122571
EGFR	1956	11.122326	12.333595
CDX4	1046	10.933424	9.588729
ISLR	3671	10.854443	9.725897
TWIST2	117581	10.853075	10.129753
VEGFA	7422	10.833399	10.087871
CTGF	1490	10.809845	11.98555
FZD7	8324	10.711324	9.901575
KRT85	3891	10.621079	9.606193
CCND1	595	10.543621	10.14267
TLE1	7088	10.343489	9.271956
CDX1	1044	10.329419	9.136879
KRT8	3856	10.267347	8.319682
NRP1	8829	10.246916	9.627893
DKK1	22943	10.211538	10.979951
IRS1	3667	10.175792	10.3609915
MMP2	4313	10.153262	9.412593
IKBK	8517	10.132635	9.295626
TIAM1	7074	10.117085	11.627998

(Continued)

Table 1 (Continued)

Gene	ID	Normalized intensity	
		Control	FH535
<i>EGR1</i>	1958	10.007974	8.180263
<i>MET</i>	4233	9.986441	12.74971
<i>BGLAP</i>	632	9.971276	9.414629
<i>VEGFC</i>	7424	9.923567	10.21814
<i>AHR</i>	196	9.886938	11.936481
<i>CACNA1G</i>	8913	9.812038	8.560494
<i>KRT15</i>	3866	9.7214575	8.709181
<i>PPAP2B</i>	8613	9.718731	9.956581
<i>KRT86</i>	3892	9.707824	9.012362
<i>KRT23</i>	25984	9.573925	7.977122
<i>GBX2</i>	2637	9.409858	9.626151
<i>KRT39</i>	390792	9.284486	7.929165
<i>WNT3A</i>	89780	9.275467	8.68014
<i>PLAUR</i>	5329	9.265003	8.37788
<i>ID2</i>	3398	9.226584	8.999163
<i>MAEA</i>	10296	9.087043	8.91366
<i>DAB2</i>	1601	9.034534	10.517419
<i>ETS2</i>	2114	8.999426	10.445461
<i>KRT31</i>	3881	8.998071	7.96933
<i>TNFRSF11A</i>	8792	8.943393	9.029845
<i>RET</i>	5979	8.9224615	7.809108
<i>UBXN6</i>	80700	8.850218	7.6966906
<i>STRA6</i>	64220	8.746183	7.1663184
<i>KLF5</i>	688	8.6543455	8.714795
<i>KRT4</i>	3851	8.640165	7.6698284
<i>UBXN4</i>	23190	8.607909	10.505396
<i>LEF1</i>	51176	8.601926	9.380911
<i>KRT76</i>	51350	8.571253	7.397269
<i>UBXN2B</i>	137886	8.2286415	9.982969
<i>UBXN11</i>	91544	8.179481	7.272692
<i>LRP1</i>	4035	8.175423	6.988433
<i>UBXN2A</i>	165324	8.133479	7.9562063
<i>KRT9</i>	3857	8.110517	7.0731263
<i>EDA</i>	1896	8.09645	7.4072337
<i>KRT32</i>	3882	8.087603	7.7537346
<i>FGF4</i>	2249	7.9492774	6.5977035
<i>KRT3</i>	3850	7.8908534	8.469248
<i>UBXN8</i>	7993	7.86574	9.013798
<i>SIX1</i>	6495	7.818405	7.9264607
<i>FOXN1</i>	8456	7.7998743	6.8640747
<i>ETV6</i>	2120	7.7085342	7.0067773
<i>KRT1</i>	3848	7.5221066	6.7497764
<i>IL8</i>	3576	7.501872	6.6113296
<i>NTRK2</i>	4915	7.497469	7.1365094
<i>RUNX2</i>	860	7.4688272	8.628798
<i>MMP11</i>	4320	7.460847	7.2920337
<i>CDH1</i>	999	7.3595057	7.319695
<i>TCF7L2</i>	6934	7.3556123	8.6040535
<i>KRT78</i>	196374	7.349466	6.8676143
<i>TCF7</i>	6932	7.270456	7.664296
<i>SMO</i>	6608	7.222788	7.0400887
<i>EFNB2</i>	1948	7.1960526	7.26771
<i>CLDN1</i>	9076	7.1643777	8.943991
<i>KRT33A</i>	3883	7.121948	6.808277
<i>VCAN</i>	1462	7.045421	6.763195
<i>MMP9</i>	4318	7.0101504	6.7540355
<i>DLL1</i>	28514	6.969655	6.5782347
<i>KRT13</i>	3860	6.949356	5.971072
<i>IGF2</i>	3481	6.933426	6.170534

(Continued)

Table 1 (Continued)

Gene	ID	Normalized intensity	
		Control	FH535
<i>KRT26</i>	353288	6.869997	6.697632
<i>TNFRSF9</i>	3604	6.862919	6.6031585
<i>KRT74</i>	121391	6.778076	6.538765
<i>TWIST1</i>	7291	6.765423	6.105777
<i>NRCAM</i>	4897	6.677019	6.7818675
<i>FGF9</i>	2254	6.6647215	5.7855196
<i>TNFRSF11B</i>	4982	6.6092443	6.618697
<i>CHL1</i>	10752	6.6082654	6.3569694
<i>KRT34</i>	3885	6.601664	6.199431
<i>KRT6A</i>	3853	6.536037	5.9656916
<i>EDN1</i>	1906	6.476451	6.7537594
<i>NOS2</i>	4843	6.425461	6.333558
<i>GDF5</i>	8200	6.3569694	6.3291264
<i>CCND2</i>	894	6.3239446	5.996339
<i>DLK1</i>	8788	6.2332454	6.884508
<i>KRT37</i>	8688	5.971611	5.881136
<i>IL6</i>	3569	5.7313643	5.9466343
<i>SOX2</i>	6657	5.6166873	6.7975965
<i>TGFB3</i>	7043	5.5891886	6.0552535
<i>KRT35</i>	3886	5.5883365	6.3580856
<i>PTGS2</i>	5743	5.5262737	7.601541
<i>BTRC</i>	8945	5.3152456	7.7473273

downregulated the protein level of total β -catenin in the PANC-1 cells, which differed from the results of most previous studies.¹⁰ This cell type-dependent downregulation of β -catenin could have been due to the stabilization of axin, which suppresses β -catenin.¹¹ Axin is characterized as a tumor-suppressor gene, and it plays a key role in inhibiting the canonical Wnt pathway by forming molecular complexes with other proteins such as GSK-3 β and adenomatous polyposis coli (APC).³⁸ Whether or not β -catenin expression was inhibited, the luciferase reporter assay proved that transcriptional activity of β -catenin pathway was decreased, which was consistent with previous study findings.¹⁰

Metastasis, the leading cause of cancer-related death, is a complex process comprising several steps, all of which we found were affected by FH535. First, FH535 inhibited pancreatic cancer cell migration. Microarray analyses revealed that FH535 altered the expression of several migration-related genes, which participate in focal adhesion, adhesion junctions, tight junctions, and/or motility regulation. Among these genes, the focal adhesion-related gene *PTEN*, considered “the most highly mutated tumor-suppressor gene in the post-p53 era”,³⁹ plays a role in controlling cell migration.⁴⁰ The loss of PTEN protein expression or function has been reported in many human cancers, including ovarian, endometrial, and prostate carcinoma; breast cancer; and primary gastrointestinal stromal tumor.^{41,42} We also found that FH535 downregulated the adhesion junction-related gene *TLN1*,

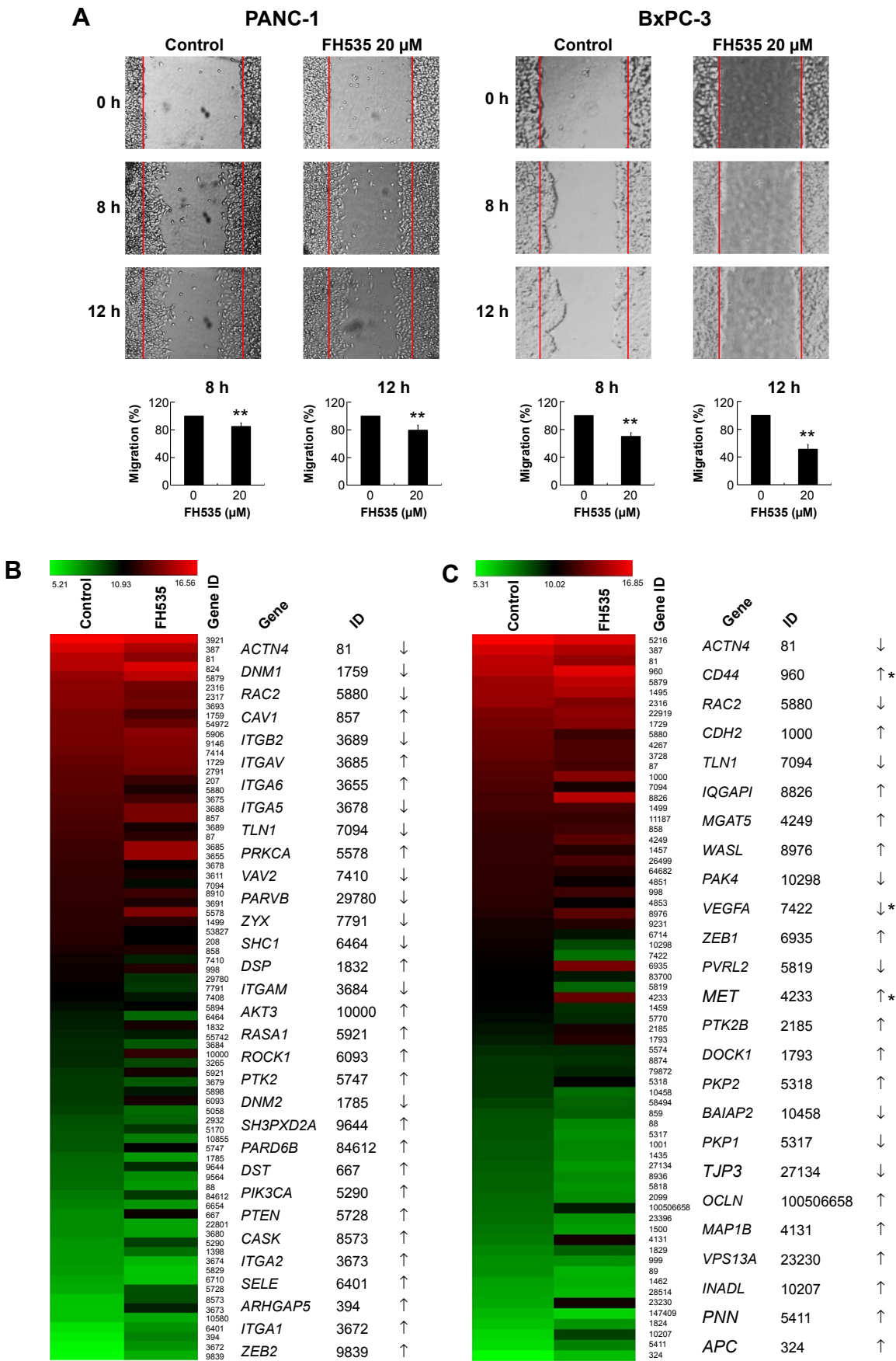


Figure 2 (Continued)

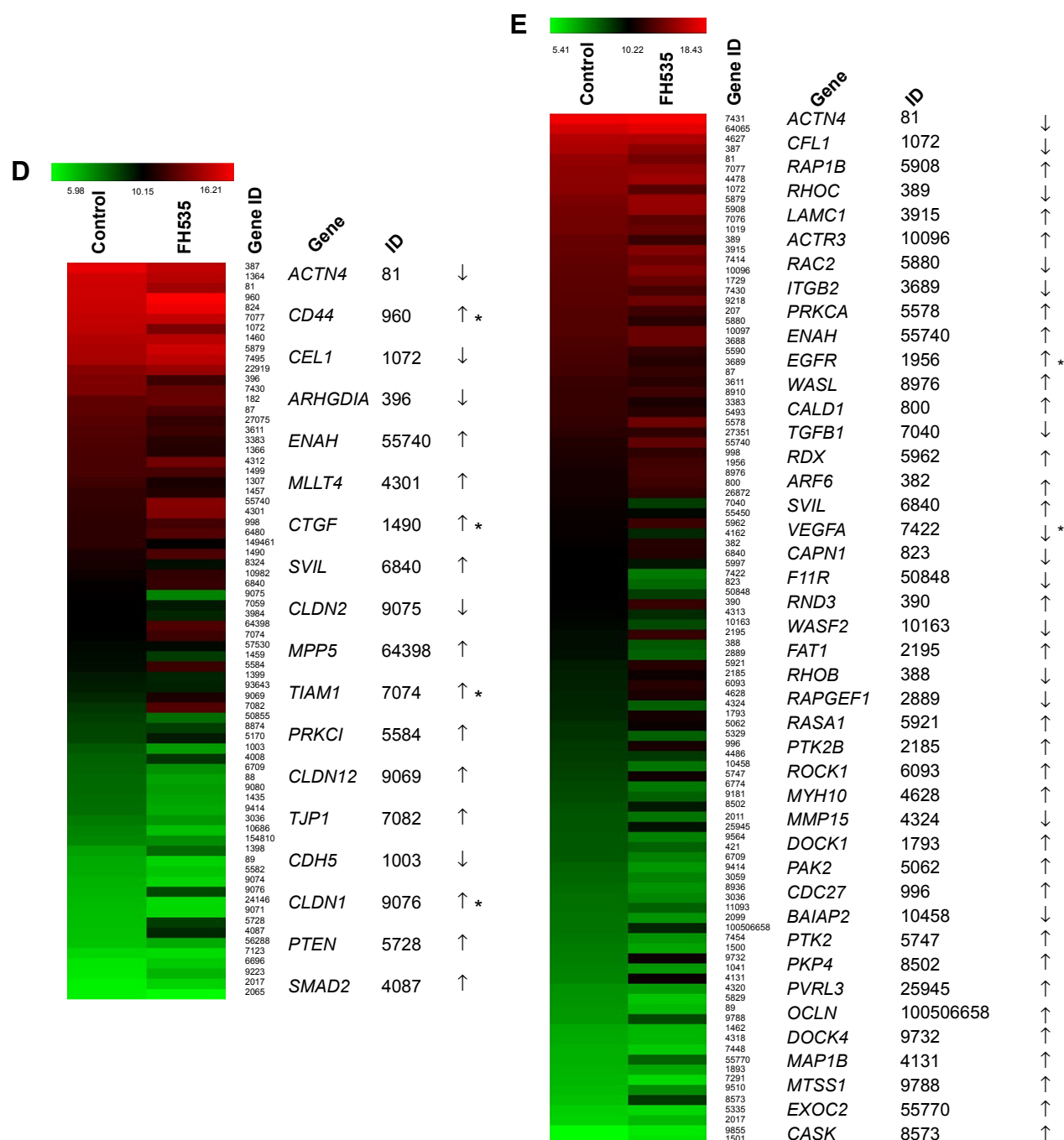


Figure 2 FH535 inhibited pancreatic cancer cell migration.

Notes: (A) Time-dependent inhibition by FH535 of PANC-1 and BxPC-3 cell migration. $**P < 0.01$, significant differences vs the respective control groups. Microarray analysis of (B) focal adhesion-related, (C) adhesion junction-related, (D) tight junction-related, and (E) cell motility-related gene expression regulation upon FH535 treatment. Up and down arrows indicate gene expression significantly upregulated or downregulated, respectively, by twofold. Asterisks indicate genes downstream of the Wnt/ β -catenin pathway.

Abbreviation: h, hours.

which encodes a cytoskeletal protein that is concentrated in areas of cell–substratum and cell–cell contact. The encoded protein plays a significant role in actin filament assembly and in the spread and migration of various cell types.^{43,44} TLN1 is codistributed with integrins in the cell surface membrane, aiding the attachment of adherent cells to extracellular

matrices and lymphocytes to other cells. In our study, tight junction protein 1 (TJP1), which plays a critical role in cell–cell interaction, proliferation, and differentiation, was upregulated. TJP1 is an important marker of tight junction integrity, which is disrupted in many highly invasive cancers; upregulated TJP1 correlates with favorable survival

Table 2 Microarray analysis of focal adhesion–related gene expression regulation upon FH535 treatment

Gene	ID	Normalized intensity	
		Control	FH535
RPSA	3921	16.551584	16.069508
RHOA	387	15.761177	14.786651
ACTN4	81	15.032014	14.01403
CAPN2	824	14.947017	15.841314
RAC1	5879	14.251518	15.113209
FLNA	2316	14.083586	13.488903
FLNB	2317	13.958575	13.296808
ITGB5	3693	13.888797	13.484464
DNM1	1759	13.640091	12.518821
TMEM132A	54972	13.622586	13.150153
RAP1A	5906	13.5597315	14.039375
HGS	9146	13.533683	13.846248
VCL	7414	13.376745	13.681126
DIAPH1	1729	13.16062	13.659487
GNG11	2791	13.022779	13.403848
AKT1	207	12.957863	12.259176
RAC2	5880	12.955015	11.604415
ITGA3	3675	12.797894	12.391577
ITGB1	3688	12.738785	13.636554
CAV1	857	12.61244	13.617725
ITGB2	3689	12.546266	11.473748
ACTN1	87	12.409878	11.967234
ITGAV	3685	12.278682	14.3424
ITGA6	3655	12.273888	14.392418
ITGA5	3678	12.169847	10.866323
ILK	3611	12.11682	11.583433
TLN1	7094	12.096641	10.645829
SGCE	8910	12.047686	12.282321
ITGB4	3691	11.982763	11.56935
PRKCA	5578	11.918201	13.803304
CTNNB1	1499	11.900537	11.841962
FXYD5	53827	11.859393	10.980669
AKT2	208	11.791592	10.995004
CAV2	858	11.534644	11.731664
VAV2	7410	11.322939	10.17948
CDC42	998	11.250544	11.791042
PARVB	29780	11.224628	9.830263
ZYX	7791	10.997072	9.663998
VASP	7408	10.877319	10.418066
RAF1	5894	10.594473	10.865986
SHC1	6464	10.287678	8.595637
DSP	1832	10.226259	11.500326
PARVA	55742	10.0804615	10.301352
ITGAM	3684	10.003317	8.889115
AKT3	10000	9.999831	12.071189
HRAS	3265	9.972342	9.272375
PDPK1	5170	9.005413	9.698432
HPSE	10855	8.978405	8.067395
PTK2	5747	8.939062	10.820772
DNM2	1785	8.613899	7.43392
SH3PXD2A	9644	8.566784	9.949804
BCAR1	9564	8.529809	7.7692404
ACTN2	88	8.437073	7.474538
PARD6B	84612	8.172608	9.636746
SOS1	6654	7.9648976	7.5355105
DST	667	7.7908773	11.245214

(Continued)

Table 2 (Continued)

Gene	ID	Normalized intensity	
		Control	FH535
ITGA11	22801	7.7725782	7.250522
ITGA9	3680	7.725706	7.2797456
PIK3CA	5290	7.546133	9.475706
CRK	1398	7.5114365	8.404298
ITGA2B	3674	7.474538	6.8249826
PXN	5829	7.426979	6.493304
SPTB	6710	7.143782	6.598218
PTEN	5728	7.0376005	9.120998
CASK	8573	6.554297	9.147331
ITGA2	3673	6.538141	10.171594
SORBS1	10580	6.5160394	7.080136
SELE	6401	5.8820415	7.629673
ARHGAP5	394	5.628543	7.9602804
ITGA1	3672	5.3547735	7.6031985
ZEB2	9839	5.2203803	6.942315

Table 3 Microarray analysis of adhesion junction–related gene expression regulation upon FH535 treatment

Gene	ID	Normalized intensity	
		Control	FH535
PFN1	5216	16.843973	16.144138
RHOA	387	15.761177	14.786651
ACTN4	81	15.032014	14.01403
CD44	960	15.006962	16.199093
RAC1	5879	14.251518	15.113209
CTNNA1	1495	14.209974	14.654735
FLNA	2316	14.083586	13.488903
MAPRE1	22919	13.413141	13.8757925
DIAPH1	1729	13.16062	13.659487
RAC2	5880	12.955015	11.604415
CD99	4267	12.8705635	12.11682
JUP	3728	12.776809	12.098349
ACTN1	87	12.409878	11.967234
CDH2	1000	12.27524	13.657263
TLN1	7094	12.096641	10.645829
IQGAP1	8826	11.903805	15.008826
CTNNB1	1499	11.900537	11.841962
PKP3	11187	11.572304	11.483009
CAV2	858	11.534644	11.731664
MGAT5	4249	11.399225	12.44798
CSNK2A1	1457	11.389523	10.994029
PLEK2	26499	11.380254	12.049034
ANAPC1	64682	11.330902	11.025982
NOTCH1	4851	11.311136	10.345143
CDC42	998	11.250544	11.791042
NOTCH2	4853	11.125797	10.202223
WASL	8976	10.930079	12.483249
DLG5	9231	10.567565	11.019769
SRC	6714	10.48147	9.648777
PAK4	10298	10.446864	8.676079
VEGFA	7422	10.250756	7.901348
ZEB1	6935	10.177025	13.283847
JAM3	83700	10.084784	9.556893
PVRL2	5819	10.018614	8.147698

(Continued)

Table 3 (Continued)

Gene	ID	Normalized intensity	
		Control	FH535
MET	4233	9.986441	12.74971
CSNK2A2	1459	9.960693	9.169151
PTPN1	5770	9.82763	9.271097
PTK2B	2185	9.636893	10.68203
DOCK1	1793	9.48097	11.021774
MAPK1	5594	9.240688	9.218932
ARHGEF7	8874	9.037083	9.147919
CBLL1	79872	9.0251875	9.311203
PKP2	5318	9.022291	10.025781
BAIAP2	10458	9.018734	8.004229
JAM2	58494	8.789471	8.162707
CAV3	859	8.535716	8.229119
ACTN2	88	8.437073	7.474538
PKP1	5317	8.423988	7.3570046
CDH3	1001	8.389479	7.50349
CSF1	1435	8.360545	7.4550886
TJP3	27134	8.295799	7.207067
WASF1	8936	8.178464	7.4462004
PVRL1	5818	8.152037	7.283169
ESR1	2099	8.048168	7.405365
OCN	100506658	8.036663	9.494983
PIP5K1C	23396	7.9606485	7.254657
CTNND1	1500	7.8659673	7.09317
MAP1B	4131	7.7052383	10.589897
DSG2	1829	7.513804	8.2605915
CDH1	999	7.3595057	7.319695
ACTN3	89	7.355976	6.6988516
VCAN	1462	7.045421	6.763195
DLL1	28514	6.969655	6.5782347
VPS13A	23230	6.859817	10.562696
DSG4	147409	6.608555	6.1116643
DSC2	1824	6.3962626	7.24841
INADL	10207	6.08029	8.808925
PNN	5411	5.9342465	7.5790677
APC	324	5.3153567	6.5241365
ITGA2	3673	6.538141	10.171594
SORBS1	10580	6.5160394	7.080136
SELE	6401	5.8820415	7.629673
ARHGAP5	394	5.628543	7.9602804
ITGA1	3672	5.3547735	7.6031985
ZEB2	9839	5.2203803	6.942315

Table 4 Microarray analysis of tight junction–related gene expression regulation upon FH535 treatment

Gene	ID	Normalized intensity	
		Control	FH535
RHOA	387	15.761177	14.786651
CLDN4	1364	15.11957	14.539507
ACTN4	81	15.032014	14.01403
CD44	960	15.006962	16.199093
CAPN2	824	14.947017	15.841314
TIMP2	7077	14.796619	14.858342
CFL1	1072	14.710272	13.114106
CSNK2B	1460	14.4039135	14.575101
RAC1	5879	14.251518	15.113209
CTNNA1	1495	14.209974	14.654735
MAPRE1	22919	13.413141	13.8757925
ARHGDIA	396	13.207352	11.634186

(Continued)

Table 4 (Continued)

Gene	ID	Normalized intensity	
		Control	FH535
EZR	7430	13.144885	12.566931
JAG1	182	12.427784	12.687155
ACTN1	87	12.409878	11.967234
TSPAN13	27075	12.246902	11.379381
ILK	3611	12.11682	11.583433
ICAM1	3383	12.0056095	11.118488
CLDN7	1366	11.972866	11.032687
MMP1	4312	11.905035	12.887484
CTNNA1	1499	11.900537	11.841962
COL16A1	1307	11.647751	10.777789
CSNK2A1	1457	11.389523	10.994029
ENAH	55740	11.354481	13.398125
MLLT4	4301	11.299263	13.275789
CDC42	998	11.250544	11.791042
IGF1R	3480	11.2369585	12.140446
CLDN19	149461	11.222952	10.278006
CTGF	1490	10.809845	11.98555
FZD7	8324	10.711324	9.901575
MAPRE2	10982	10.535324	11.375724
SVIL	6840	10.304885	11.463148
CLDN2	9075	10.221999	7.959734
THBS3	7059	10.1687765	9.736564
LIMK1	3984	10.151468	9.52237
MPP5	64398	10.149654	12.064446
TIAM1	7074	10.117085	11.627998
CGN	57530	10.004088	9.987757
CSNK2A2	1459	9.960693	9.169151
PRKCI	5584	9.934886	11.633633
CRKL	1399	9.737389	9.574368
TJAP1	93643	9.66933	9.609078
CLDN12	9069	9.506469	10.83943
TJPI	7082	9.28694	12.134832
PARD6A	50855	9.12321	8.362814
ARHGEF7	8874	9.037083	9.147919
PDPK1	5170	9.005413	9.698432
CDH5	1003	8.708324	7.5856657
LMO7	4008	8.558113	9.277104
SPTAN1	6709	8.494044	7.7864056
ACTN2	88	8.437073	7.474538
CLDN9	9080	8.4181795	7.5940213
CSF1	1435	8.360545	7.4550886
TJP2	9414	8.343918	7.3491254
HAS1	3036	8.124433	7.6573296
CLDN16	10686	7.9999046	7.022292
AMOTL1	154810	7.8963585	7.8100796
CRK	1398	7.5114365	8.404298
ACTN3	89	7.355976	6.6988516
PRKCG	5582	7.321149	6.9112835
CLDN6	9074	7.220466	6.6578355
CLDN1	9076	7.1643777	8.943991
CLDN15	24146	7.0927997	6.5795236
CLDN10	9071	7.0557775	6.613464
PTEN	5728	7.0376005	9.120998
SMAD2	4087	6.9688606	9.496367
PARD3	56288	6.94016	7.33421
CLEC3B	7123	6.6491346	6.5587797
SPPI	6696	6.37645	6.842924
MAGI1	9223	6.3656254	7.168139
CTTN	2017	6.2022476	6.6959023
ERBB3	2065	6.178696	5.9926624

Table 5 Microarray analysis of cell motility-related gene expression regulation upon FH535 treatment

Gene	ID	Normalized intensity	
		Control	FH535
VIM	7431	18.111416	18.417988
PERP	64065	17.034954	17.530819
MYH9	4627	16.01196	15.906586
RHOA	387	15.761177	14.786651
ACTN4	81	15.032014	14.01403
TIMP2	7077	14.796619	14.858342
MSN	4478	14.751841	15.357616
CFLI	1072	14.710272	13.114106
RAC1	5879	14.251518	15.113209
RAP1B	5908	14.023661	15.037672
TIMP1	7076	13.919523	13.2338505
CDK4	1019	13.87332	13.635977
RHOC	389	13.521647	12.094296
LAMC1	3915	13.492421	14.51922
VCL	7414	13.376745	13.681126
ACTR3	10096	13.228158	14.45616
DIAPH1	1729	13.16062	13.659487
EZR	7430	13.144885	12.566931
VAPA	9218	13.089962	13.857084
AKT1	207	12.957863	12.259176
RAC2	5880	12.955015	11.604415
ACTR2	10097	12.94824	13.651513
ITGB1	3688	12.738785	13.636554
PRKCZ	5590	12.597843	11.836956
ITGB2	3689	12.546266	11.473748
ACTN1	87	12.409878	11.967234
ILK	3611	12.11682	11.583433
SGCE	8910	12.047686	12.282321
ICAM1	3383	12.0056095	11.118488
PPL	5493	11.998627	11.51075
PRKCA	5578	11.918201	13.803304
PPPDE2	27351	11.624274	11.774211
ENAH	55740	11.354481	13.398125
CDC42	998	11.250544	11.791042
EGFR	1956	11.122326	12.333595
WASL	8976	10.930079	12.483249
CALD1	800	10.921519	12.294691
STEAP1	26872	10.895491	11.820029
TGFB1	7040	10.7152	9.03388
CAMK2N1	55450	10.587699	10.065469
RDX	5962	10.522251	12.191257
MCAM	4162	10.452353	9.462444
ARF6	382	10.415711	11.52632
SVIL	6840	10.304885	11.463148
RGS2	5997	10.257294	9.80196
VEGFA	7422	10.250756	7.901348
CAPN1	823	10.239203	8.216266
FILR	50848	10.234683	9.044022
RND3	390	10.199277	12.088578
MMP2	4313	10.153262	9.412593
WASF2	10163	10.085579	8.826545
FAT1	2195	9.970972	12.042841
RHOB	388	9.965946	8.545685
RAPGEF1	2889	9.903289	8.354535
RASA1	5921	9.702747	11.502001
PTK2B	2185	9.636893	10.68203
ROCK1	6093	9.603488	11.484902

(Continued)

Table 5 (Continued)

Gene	ID	Normalized intensity	
		Control	FH535
MYH10	4628	9.5496025	11.096066
MMP15	4324	9.533566	8.395943
DOCK1	1793	9.48097	11.021774
PAK2	5062	9.287464	10.61245
PLAUR	5329	9.265003	8.37788
CDC27	996	9.129515	11.077047
MST1R	4486	9.085802	9.12538
BAIAP2	10458	9.018734	8.004229
PTK2	5747	8.939062	10.820772
STAT3	6774	8.847785	7.9192953
ARHGEF2	9181	8.798216	8.383045
PKP4	8502	8.663319	9.734335
MARK2	2011	8.612933	8.00314
PVRL3	25945	8.582907	9.851074
BCAR1	9564	8.529809	7.7692404
ARVCF	421	8.524339	8.364944
SPTAN1	6709	8.494044	7.7864056
TJP2	9414	8.343918	7.3491254
HCLS1	3059	8.263556	7.7210197
WASF1	8936	8.178464	7.4462004
HAS1	3036	8.124433	7.6573296
ADAMTS13	11093	8.074093	8.375932
ESR1	2099	8.048168	7.405365
OCLN	100506658	8.036663	9.494983
WAS	7454	7.9598556	7.412658
CTNND1	1500	7.8659673	7.09317
DOCK4	9732	7.829811	10.702755
CDSN	1041	7.738298	7.3062844
MAP1B	4131	7.7052383	10.589897
MMP11	4320	7.460847	7.2920337
PXN	5829	7.426979	6.493304
ACTN3	89	7.355976	6.6988516
MTSS1	9788	7.3144355	8.826939
VCAN	1462	7.045421	6.763195
MMP9	4318	7.0101504	6.7540355
VTN	7448	6.8925853	6.3992944
EXOC2	55770	6.8692775	8.335709
ECM1	1893	6.8224096	7.0186477
TWIST1	7291	6.765423	6.105777
ADAMTS1	9510	6.670437	7.5566187
CASK	8573	6.554297	9.147331
PLCG1	5335	6.326862	6.175169
CTTN	2017	6.2022476	6.6959023
FARP2	9855	5.4352922	5.775334
CTNND2	1501	5.4170265	5.9111185

in breast cancer and gastrointestinal stromal tumor.^{45,46}

The motility-related gene *VEGFA* significantly increases the motility of pancreatic cancer cells. The vascular endothelial growth factor/vascular endothelial growth factor receptor (VEGF/VEGFR) inhibitors bevacizumab and sunitinib significantly decrease pancreatic cancer cell motility.⁴⁷ In our study, FH535 not only suppressed *VEGFA* expression

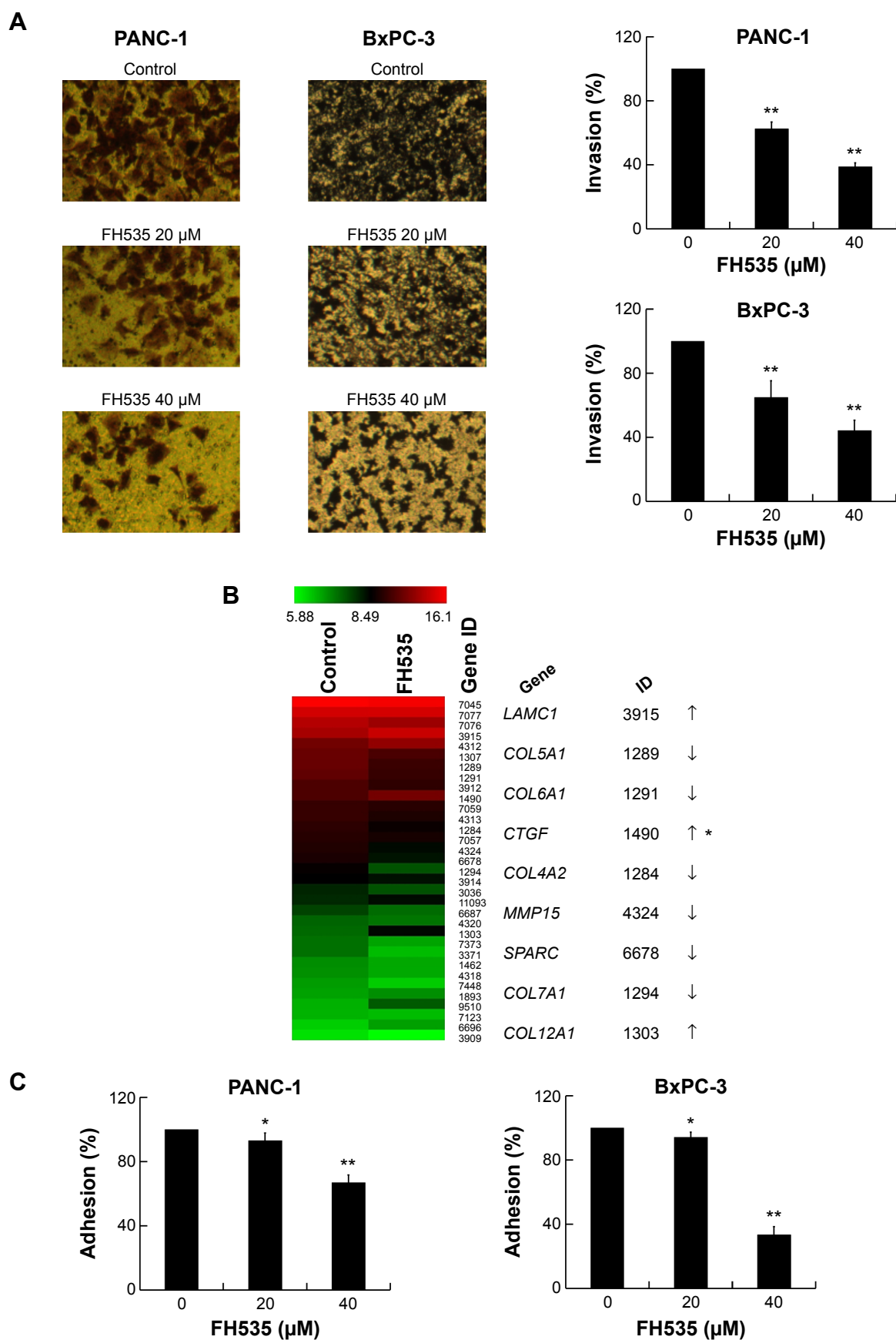


Figure 3 (Continued)

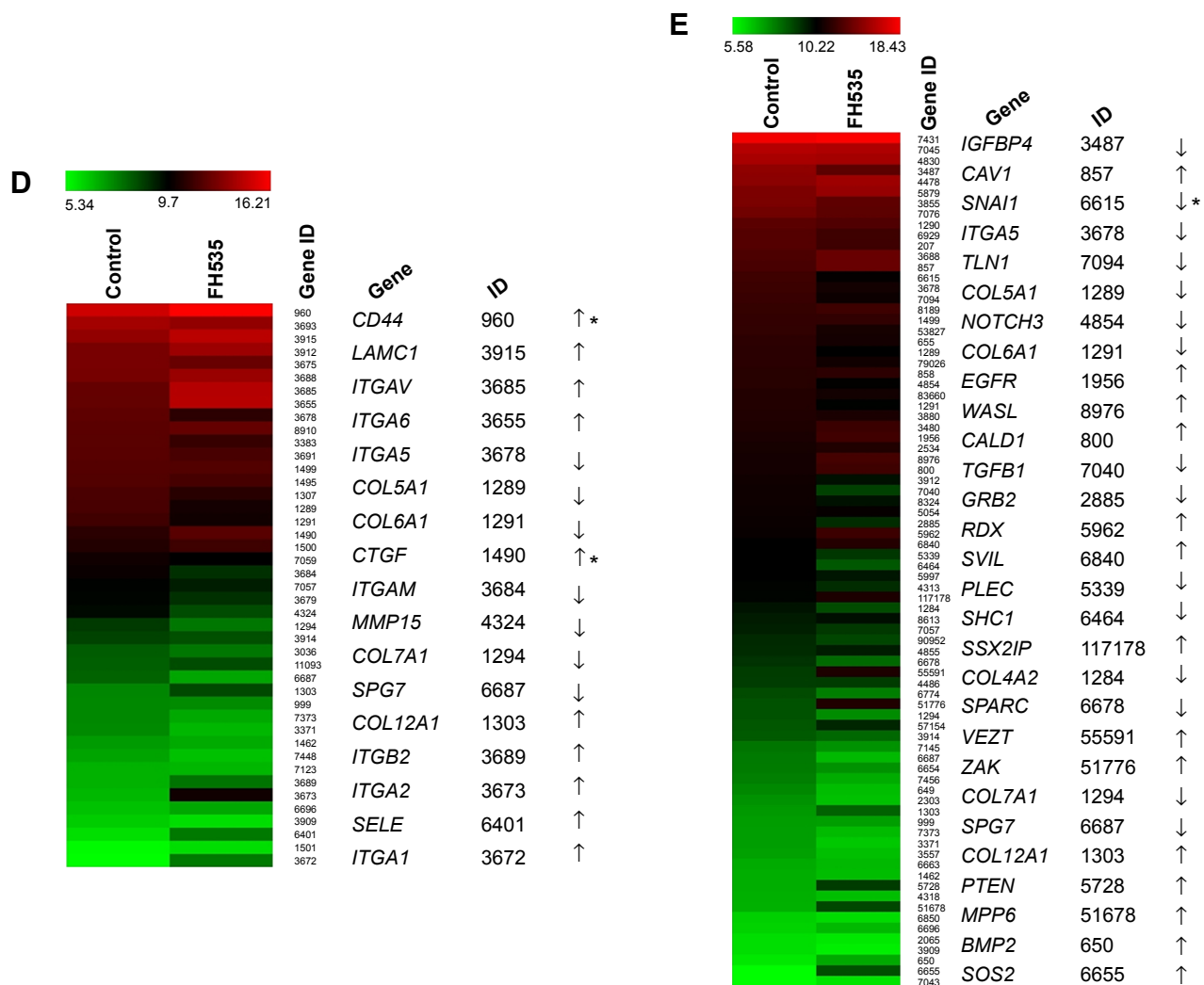


Figure 3 FH535 inhibited pancreatic cancer cell invasion.

Notes: (A) Dose-dependent inhibition by FH535 of PANC-1 and BxPC-3 cell invasion. (B) Microarray analysis of extracellular matrix degradation-related gene expression regulation upon FH535 treatment. (C) Dose-dependent inhibition by FH535 of PANC-1 and BxPC-3 cell adhesion. * $P < 0.05$, ** $P < 0.01$, significant differences vs the respective control groups. (D) Microarray analysis of adhesion molecule-related gene expression regulation upon FH535 treatment. (E) Microarray analysis of EMT-related gene expression regulation upon FH535 treatment. Up and down arrows indicate gene expression significantly upregulated or downregulated, respectively, by twofold. Asterisks indicate genes downstream of the Wnt/ β -catenin pathway.

Abbreviation: EMT, epithelial–mesenchymal transition.

but also inhibited cell motility, suggesting the involvement of a similar mechanism.

To establish metastasis, tumor cells must traverse the basement membrane to reach the connective tissues. Accordingly, we investigated the anti-invasive effect of FH535. The Transwell assay proved that FH535 inhibited invasion. In vitro invasion can be divided into several steps, including matrix adhesion, matrix degradation, and EMT. We analyzed the expression of the genes involved in these steps using microarray and found that FH535 significantly downregulated the cell adhesion molecule ITGA5; *ITGA5* knockdown results in decreased adhesion in pancreatic cancer cells.⁴⁸ The ability of matrix metalloproteinases (MMPs) to degrade

extracellular matrix proteins has been well characterized; therefore, they have been studied extensively to elucidate their involvement in both tumor development and progression. Different MMPs play different roles in tumorigenesis. MMP15 appears to be upregulated during colorectal tumorigenesis, and past research has shown stromal localization of MMP15 in the early phases of neoplastic transformation in colorectal cancer.⁴⁹ In our study, FH535 downregulated MMP15. Epithelial cells are characterized by well-developed junctions and apical–basolateral polarization; on the contrary, mesenchymal cells lack polarization due to the loss of an organized junctional layer. Cell metastasis is correlated with EMT. In the present study, FH535

Table 6 Microarray analysis of extracellular matrix degradation-related gene expression regulation upon FH535 treatment

Gene	ID	Normalized intensity	
		Control	FH535
TGFB1	7045	16.09069	15.894443
TIMP2	7077	14.796619	14.858342
TIMP1	7076	13.919523	13.2338505
LAMC1	3915	13.492421	14.51922
MMP1	4312	11.905035	12.887484
COL16A1	1307	11.647751	10.777789
COL5A1	1289	11.607744	10.272581
COL6A1	1291	11.396863	10.174638
LAMB1	3912	10.813978	9.924841
CTGF	1490	10.809845	11.98555
THBS3	7059	10.1687765	9.736564
MMP2	4313	10.153262	9.412593
COL4A2	1284	9.866227	8.850218
THBS1	7057	9.663341	9.193558
MMP15	4324	9.533566	8.395943
SPARC	6678	9.32407	8.289816
COL7A1	1294	8.711706	7.6560946
LAMB3	3914	8.550647	8.319239
HAS1	3036	8.124433	7.6573296
ADAMTS13	11093	8.074093	8.375932
SPG7	6687	7.799603	7.3888316
MMP11	4320	7.460847	7.2920337
COL12A1	1303	7.404812	8.422412
COL14A1	7373	7.3424816	6.805993
TNC	3371	7.329479	6.564947
VCAN	1462	7.045421	6.763195
MMP9	4318	7.0101504	6.7540355
VTN	7448	6.8925853	6.3992944
ECM1	1893	6.8224096	7.0186477
ADAMTS1	9510	6.670437	7.5566187
CLEC3B	7123	6.6491346	6.5587797
SPP1	6696	6.37645	6.842924
LAMA3	3909	6.1783895	5.889333

downregulated Snail, which is upregulated during EMT.⁵⁰ In human colorectal cancer cells, overexpression of Snail induces not only EMT but also a cancer stem cell-like phenotype, which enhances cell migration and invasion in vitro and increases metastasis formation in vivo.⁵¹ Snail also plays an essential role in human pancreatic cancer progression and metastasis.^{52,53} In the clinical setting, overexpression of Snail was previously associated with poorer prognosis and a more invasive phenotype in many malignancies.^{54–56} We also detected the downregulation of TGFB1, a classic EMT stimulator.⁵⁷ TGFB1 overexpression is associated with early recurrence following resection and decreased survival,⁵⁸ consistent with our study, the suppression of TGFB1 activity in immune-deficient orthotopic mouse models of pancreatic cancer attenuated tumor growth and metastasis.^{59,60}

Besides metastasis, FH535 also induced G2/M arrest and inhibited pancreatic cancer cell proliferation. FH535

Table 7 Microarray analysis of adhesion molecule-related gene expression regulation upon FH535 treatment

Gene	ID	Normalized intensity	
		Control	FH535
CD44	960	15.006962	16.199093
ITGB5	3693	13.888797	13.484464
LAMC1	3915	13.492421	14.51922
LAMB1	3912	12.817556	13.73472
ITGA3	3675	12.797894	12.391577
ITGB1	3688	12.738785	13.636554
ITGAV	3685	12.278682	14.3424
ITGA6	3655	12.273888	14.392418
ITGA5	3678	12.169847	10.866323
SGCE	8910	12.047686	12.282321
ICAM1	3383	12.0056095	11.118488
ITGB4	3691	11.982763	11.56935
CTNNB1	1499	11.900537	11.841962
CTNNA1	1495	11.841962	11.517105
COL16A1	1307	11.647751	10.777789
COL5A1	1289	11.607744	10.272581
COL6A1	1291	11.396863	10.174638
CTGF	1490	10.809845	11.98555
CTNND1	1500	10.622252	11.350482
THBS3	7059	10.1687765	9.736564
ITGAM	3684	10.003317	8.889115
THBS1	7057	9.663341	9.193558
ITGA7	3679	9.627002	8.878363
MMP15	4324	9.533566	8.395943
COL7A1	1294	8.711706	7.6560946
LAMB3	3914	8.550647	8.319239
HAS1	3036	8.124433	7.6573296
ADAMTS13	11093	8.074093	8.375932
SPG7	6687	7.990712	6.850328
COL12A1	1303	7.404812	8.422412
CDH1	999	7.3595057	7.319695
COL14A1	7373	7.3424816	6.805993
TNC	3371	7.329479	6.564947
VCAN	1462	7.045421	6.763195
VTN	7448	6.8925853	6.3992944
CLEC3B	7123	6.6491346	6.5587797
ITGB2	3689	6.6435785	7.713477
ITGA2	3673	6.538141	10.171594
SPP1	6696	6.37645	6.842924
LAMA3	3909	6.1783895	5.889333
SELE	6401	5.8820415	7.629673
CTNND2	1501	5.4170265	5.9111185
ITGA1	3672	5.3547735	7.6031985

significantly upregulated the G2/M regulator gene *BCCIP* while downregulating the cell cycle regulatory genes *CCNG1* and *SERTAD1*. Human BCCIP, a protein that interacts with BRCA2 and CDKN1A (Cip1, p21), has been implicated in many cellular processes, including cell cycle regulation, DNA recombination and damage repair, telomere maintenance, embryonic development, and genomic stability.^{61–63}

Table 8 Microarray analysis of EMT-related gene expression regulation upon FH535 treatment

Gene	ID	Normalized intensity	
		Control	FH535
VIM	7431	18.111416	18.417988
TGFB1	7045	16.09069	15.894443
NME1	4830	15.692858	15.573043
IGFBP4	3487	14.852157	13.246835
MSN	4478	14.751841	15.357616
RAC1	5879	14.251518	15.113209
KRT7	3855	14.184294	13.285099
TIMP1	7076	13.919523	13.2338505
COL5A2	1290	13.175857	12.833253
TCF3	6929	13.00084	12.29279
AKT1	207	12.957863	12.259176
ITGB1	3688	12.738785	13.636554
CAV1	857	12.61244	13.617725
SNAIL	6615	12.28132	10.385736
ITGA5	3678	12.169847	10.866323
TLN1	7094	12.096641	10.645829
SYMPK	8189	11.942529	12.312602
CTNNA1	1499	11.900537	11.841962
FXYD5	53827	11.859393	10.980669
BMP7	655	11.688513	10.938241
COL5A1	1289	11.607744	10.272581
AHNAK	79026	11.605762	10.785921
CAV2	858	11.534644	11.731664
NOTCH3	4854	11.523583	10.370972
TLN2	83660	11.404076	10.886059
COL6A1	1291	11.396863	10.174638
KRT19	3880	11.289505	11.101922
IGF1R	3480	11.2369585	12.140446
EGFR	1956	11.122326	12.333595
FYN	2534	10.966112	11.325876
WASL	8976	10.930079	12.483249
CALD1	800	10.921519	12.294691
LAMB1	3912	10.813978	9.924841
TGFB1	7040	10.7152	9.03388
FZD7	8324	10.711324	9.901575
SERPINE1	5054	10.639182	10.452353
GRB2	2885	10.605613	9.416897
RDX	5962	10.522251	12.191257
SVIL	6840	10.304885	11.463148
PLEC	5339	10.301559	9.204668
SHC1	6464	10.287678	8.595637
RGS2	5997	10.257294	9.80196
MMP2	4313	10.153262	9.412593
SSX2IP	117178	10.144432	11.167568
COL4A2	1284	9.866227	8.850218
PPAP2B	8613	9.718731	9.956581
THBS1	7057	9.663341	9.193558
ESAM	90952	9.472261	8.959825
NOTCH4	4855	9.433491	9.707824
SPARC	6678	9.32407	8.289816
VEZT	55591	9.128493	11.195451
MST1R	4486	9.085802	9.12538
STAT3	6774	8.847785	7.9192953
ZAK	51776	8.719432	11.337164
COL7A1	1294	8.711706	7.6560946
SMURF1	57154	8.629299	9.522539
LAMB3	3914	8.550647	8.319239
TNSI	7145	8.064375	7.5303655

(Continued)

Table 8 (Continued)

Gene	ID	Normalized intensity	
		Control	FH535
SPG7	6687	7.990712	6.850328
SOS1	6654	7.9648976	7.5355105
WIPF1	7456	7.8996034	7.0742846
BMP1	649	7.73736	6.776738
FOXO2	2303	7.5557323	6.690961
COL12A1	1303	7.404812	8.422412
CDH1	999	7.3595057	7.319695
COL14A1	7373	7.3424816	6.805993
TNC	3371	7.329479	6.564947
IL1RN	3557	7.2758436	6.734858
SOX10	6663	7.0939784	6.8492174
VCAN	1462	7.045421	6.763195
PTEN	5728	7.0376005	9.120998
MMP9	4318	7.0101504	6.7540355
MPP6	51678	6.9906545	8.912582
SYK	6850	6.4246235	6.223468
SPP1	6696	6.37645	6.842924
ERBB3	2065	6.178696	5.9926624
LAMA3	3909	6.1783895	5.889333
BMP2	650	6.0141077	7.1390386
SOS2	6655	5.6132765	8.797646
TGFB3	7043	5.5891886	6.0552535

Abbreviation: EMT, epithelial-mesenchymal transition.

BCCIP knockdown and concomitant p53 deletion causes rapid development of medulloblastomas, which have a wide spectrum of alterations involving the Sonic hedgehog pathway, consistent with the caretaker responsibility of *BCCIP* in genomic integrity.⁶⁴ *BCCIP* expression is downregulated in human ovarian cancer, renal cell carcinoma, and colorectal cancer tissues, suggesting that the gene plays a role in the pathogenesis of these cancers.⁶³ The positive expression rate and intensity of *CCNG1* in gastric carcinoma is significantly correlated with tumor differentiation. Elevated amounts of *CCNG1* are frequently detected in malignant tissue tumors, including astrocytoma; melanoma; carcinoma of the esophagus, lung, and breast; and cancer of the cervix, uterus, and ovary.⁶⁵ It plays a pivotal role in hepatocellular carcinoma metastasis and may be a novel prognostic biomarker and therapeutic target.⁶⁶ *SERTAD1* is involved in positive regulation of the cell cycle and proliferation;^{67,68} accordingly, its expression is upregulated in several tumor types.^{69,70} Studies indicate that *SERTAD1* promotes proliferation by binding to the transcription factor E2F1 and by enhancing its transcriptional activity.⁷¹ Experimental overexpression of *SERTAD1* provoked hyperproliferation,⁷² genomic instability,⁶⁸ and inhibition of apoptosis.⁷³

We demonstrated that FH535 significantly inhibits pancreatic cancer cell metastasis by suppressing migration, invasion, and adhesion and induces the accumulation of cells in the G2/M phase to suppress proliferation. These results

suggest that FH535 is a potential candidate for pancreatic cancer treatment. Some of the identified genes that responded to FH535 are well-established direct targets of the Wnt/ β -catenin pathway. However, it has not been proven that the other identified genes are located downstream of the pathway. FH535 might affect the expression of these genes through the Wnt/ β -catenin pathway indirectly or in

a β -catenin independent manner. In fact, FH535 not only antagonizes β -catenin/TCF-mediated transcription but also inhibits recruitment of the coactivators glucocorticoid receptor-interacting protein 1 (GRIP1) and β -catenin to peroxisome proliferator-activated receptor (PPAR) δ and PPAR γ ,¹⁰ suggesting that these mechanisms could also be involved in the anti-cancer effect of FH535.

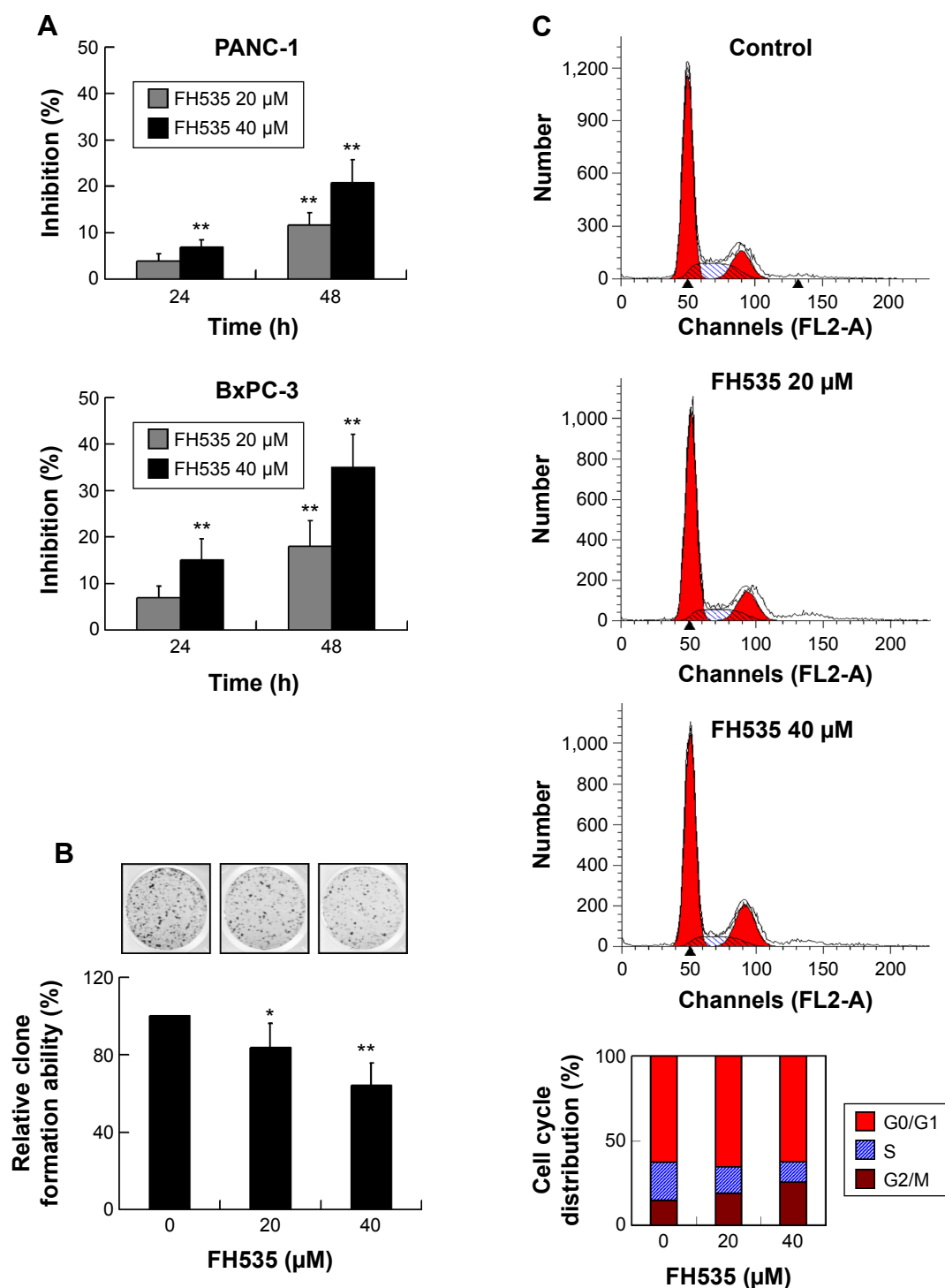


Figure 4 (Continued)

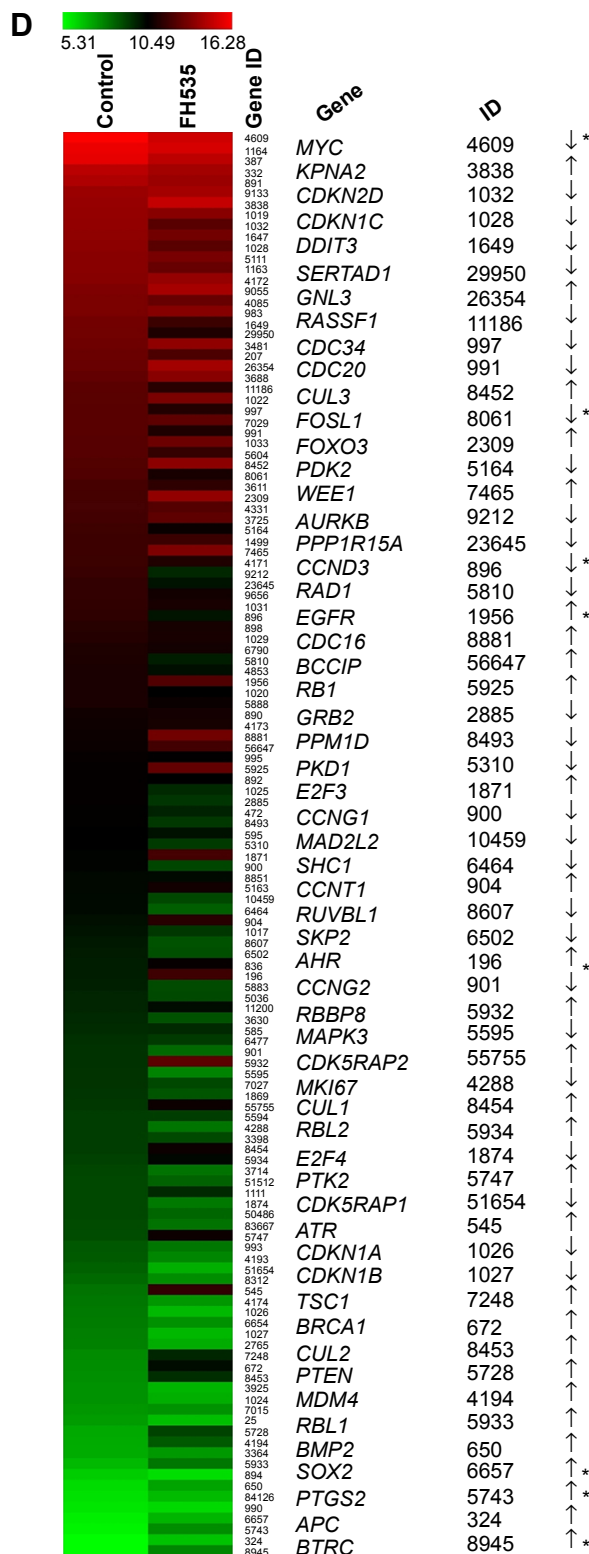


Figure 4 Inhibitory effect of FH535 on pancreatic cancer cell growth.

Notes: (A) Dose- and time-dependent inhibition by FH535 of PANC-1 and BxPC-3 cell growth. (B) Dose-dependent inhibition by FH535 of the clone formation ability of BxPC-3 cells. * $P < 0.05$, ** $P < 0.01$, significant differences vs the respective control groups. (C) Significant dose-dependent G2/M arrest following FH535 treatment in BxPC-3 cells. (D) Microarray analysis of cell cycle-related gene expression regulation upon 20 μ M FH535 treatment. Up and down arrows indicate gene expression significantly upregulated or downregulated, respectively, by twofold. Asterisks indicate genes downstream of the Wnt/ β -catenin pathway.

Abbreviation: h, hours.

Table 9 Microarray analysis of cell cycle-related gene expression regulation upon 20 μ M FH535 treatment

Gene	ID	Normalized intensity	
		Control	FH535
MYC	4609	16.268158	15.204586
CKS2	1164	15.878164	15.394571
RHOA	387	15.761177	14.786651
BIRC5	332	14.757564	14.219355
CCNB1	891	14.478785	14.022737
CCNB2	9133	14.019871	14.271269
KPNA2	3838	13.950185	14.971469
CDK4	1019	13.87332	13.635977
CDKN2D	1032	13.839806	12.513427
GADD45A	1647	13.765451	13.130958
CDKN1C	1028	13.694702	12.537176
PCNA	5111	13.611973	13.2414665
CKS1B	1163	13.609195	12.845673
MCM3	4172	13.580797	13.911951
PRCI	9055	13.4114275	14.32471
MAD2L1	4085	13.297964	12.867024
CDK1	983	13.286596	13.600226
DDIT3	1649	13.135856	11.871853
SERTAD1	29950	13.060848	11.212
IGF2	3481	13.0203	13.799717
AKT1	207	12.957863	12.259176
GNL3	26354	12.891848	14.223899
ITGB1	3688	12.738785	13.636554
RASSF1	11186	12.559567	11.458946
CDK7	1022	12.553116	13.288865
CDC34	997	12.53036	11.302476
TFDP2	7029	12.527303	12.6644745
CDC20	991	12.526335	11.232994
CDKN3	1033	12.486179	12.966997
MAP2K1	5604	12.483637	11.714967
CUL3	8452	12.389215	13.715795
FOSL1	8061	12.344017	11.102832
ILK	3611	12.11682	11.583433
FOXO3	2309	12.095011	13.865094
MNAT1	4331	12.074865	12.456777
JUN	3725	12.038464	12.673436
PDK2	5164	11.944916	10.781894
CTNNB1	1499	11.900537	11.841962
WEE1	7465	11.894105	13.381722
MCM2	4171	11.862871	11.269842
AURKB	9212	11.800928	9.697033
PPP1R15A	23645	11.676006	10.124018
MDC1	9656	11.649198	10.940614
CDKN2C	1031	11.6150875	11.096327
CCND3	896	11.576098	10.075832
CCNE1	898	11.407219	11.045229
CDKN2A	1029	11.343829	11.097562
AURKA	6790	11.181647	10.961699
RAD1	5810	11.162613	9.890079
NOTCH2	4853	11.125797	10.202223
EGFR	1956	11.122326	12.333595
CDK5	1020	11.117936	10.542482
RAD51	5888	11.1082325	10.784544
CCNA2	890	10.911861	10.9871645
MCM4	4173	10.849212	11.05679
CDC16	8881	10.808938	13.084003

(Continued)

Table 9 (Continued)

Gene	ID	Normalized intensity	
		Control	FH535
BCCIP	56647	10.778181	12.021907
CDC25C	995	10.672214	10.564099
RBI	5925	10.640414	12.741512
CCNC	892	10.610059	10.50804
CDK9	1025	10.606858	9.6394415
GRB2	2885	10.605613	9.416897
ATM	472	10.5960865	9.790577
PPM1D	8493	10.580978	9.338833
CCND1	595	10.543621	10.14267
PKD1	5310	10.471296	9.29677
E2F3	1871	10.412796	12.061844
CCNG1	900	10.409301	9.063653
CDK5R1	8851	10.322197	10.292204
PDK1	5163	10.321034	10.933424
MAD2L2	10459	10.306548	9.040705
SHC1	6464	10.287678	8.595637
CCNT1	904	10.17827	11.456285
CDK2	1017	10.10528	9.357359
RUVBL1	8607	10.000026	8.814938
SKP2	6502	9.937107	8.872935
CASP3	836	9.893856	10.658698
AHR	196	9.886938	11.936481
RAD9A	5883	9.855825	8.961951
PA2G4	5036	9.737894	8.966842
CHEK2	11200	9.726725	10.255492
INS	3630	9.673779	8.813154
BBS4	585	9.597437	9.65494
SIAH1	6477	9.530121	9.295226
CCNG2	901	9.4692955	8.337656
RBBP8	5932	9.454372	12.631638
MAPK3	5595	9.447224	7.818405
TFDP1	7027	9.4434185	9.030092
E2F1	1869	9.397123	8.754342
CDK5RAP2	55755	9.390803	10.79269
MAPK1	5594	9.240688	9.218932
MKI67	4288	9.233824	8.092867
ID2	3398	9.226584	8.999163
CUL1	8454	9.221058	10.794849
RBL2	5934	9.160267	10.348637
JAG2	3714	9.075178	8.140677
GTSE1	51512	9.04477	8.488665
CHEK1	1111	9.04231	9.651725
E2F4	1874	9.035055	8.016477
GOS2	50486	9.032754	8.410861
SESN2	83667	8.951754	8.138044
PTK2	5747	8.939062	10.820772
CDC25A	993	8.677163	8.042739
MDM2	4193	8.622698	7.73673
CDK5RAP1	51654	8.508385	6.9220624
AXIN1	8312	8.351635	7.6164603
ATR	545	8.152882	11.634625
MCM5	4174	8.055058	7.4200873
CDKN1A	1026	8.007444	6.7135
SOS1	6654	7.9648976	7.5355105
CDKN1B	1027	7.8906517	6.7354736
GML	2765	7.8596773	6.9595275

(Continued)

Table 9 (Continued)

Gene	ID	Normalized intensity	
		Control	FH535
TSC1	7248	7.6562896	9.700143
BRCA1	672	7.620017	10.24544
CUL2	8453	7.566332	9.5496025
STMN1	3925	7.5155845	6.8102884
CDK8	1024	7.5133963	6.9160185
TERT	7015	7.4070444	7.4882307
ABL1	25	7.3099413	6.6226487
PTEN	5728	7.0376005	9.120998
MDM4	4194	6.996299	8.63818
HUS1	3364	6.976554	7.3689637
RBL1	5933	6.7265186	8.035306
CCND2	894	6.3239446	5.996339
BMP2	650	6.0141077	7.1390386
ATRIP	84126	5.912352	6.682503
CDC6	990	5.8019896	6.064807
SOX2	6657	5.6166873	6.7975965
PTGS2	5743	5.5262737	7.601541
APC	324	5.3153567	6.5241365
BTRC	8945	5.3152456	7.7473273

Acknowledgments

This study was supported by the National Natural Science Foundation of China (grant nos 81472296, 81101867, 81272542, 81200369, and 81372443), the CSPAC-Celgene Foundation, the China International Medical Foundation (grant no CIMF-F-H001-057), the Special Foundation of Clinical Medicine of Jiangsu Provincial Bureau of Science and Technology (grant no BL2014039), the Scientific Research Project of Jiangsu Provincial Bureau of Traditional Chinese Medicine (grant no L213236), the Medical Scientific Research Project of Jiangsu Provincial Bureau of Health (grant no Z201206), the Special Foundation of Wu Jieping Medical Foundation for Clinical Scientific Research (grant nos 320.6753.1225 and 320.6750.12242), the Science and Education for Health Foundation of Suzhou for Youth (grant nos SWKQ1003 and SWKQ1011), the Science and Technology Project Foundation of Suzhou (grant nos SYS201112, SYSD2012137, and SYS201335), the Science and Technology Foundation of Suzhou Xiangcheng (grant nos SZXC2012-70 and XJ201451), and a project founded by the priority academic program development of Jiangsu higher education institutions.

Disclosure

The authors report no conflicts of interest in this work.

References

1. Jemal A, Siegel R, Ward E, et al. Cancer statistics, 2006. *CA Cancer J Clin.* 2006;56(2):106–130.
2. Li D, Xie K, Wolff R, Abbruzzese JL. Pancreatic cancer. *Lancet.* 2004;363(9414):1049–1057.

3. Bosetti C, Bertuccio P, Malvezzi M, et al. Cancer mortality in Europe, 2005–2009, and an overview of trends since 1980. *Ann Oncol*. 2013; 24(10):2657–2671.
4. Cai HH, Sun YM, Miao Y, et al. Aberrant methylation frequency of TNFRSF10C promoter in pancreatic cancer cell lines. *Hepatobiliary Pancreat Dis Int*. 2011;10(1):95–100.
5. Iida J, Wilhelmson KL, Price MA, et al. Membrane type-1 matrix metalloproteinase promotes human melanoma invasion and growth. *J Invest Dermatol*. 2004;122(1):167–176.
6. Eisenmann KM, McCarthy JB, Simpson MA, et al. Melanoma chondroitin sulphate proteoglycan regulates cell spreading through Cdc42, Ack-1 and p130cas. *Nat Cell Biol*. 1999;1(8):507–513.
7. Vaid M, Prasad R, Sun Q, Katiyar SK. Silymarin targets beta-catenin signaling in blocking migration/invasion of human melanoma cells. *PLoS One*. 2011;6(7):e23000.
8. Iida J, Pei D, Kang T, et al. Melanoma chondroitin sulfate proteoglycan regulates matrix metalloproteinase-dependent human melanoma invasion into type I collagen. *J Biol Chem*. 2001;276(22): 18786–18794.
9. Clevers H. Wnt/beta-catenin signaling in development and disease. *Cell*. 2006;127(3):469–480.
10. Handeli S, Simon JA. A small-molecule inhibitor of Tcf/beta-catenin signaling down-regulates PPARgamma and PPARdelta activities. *Mol Cancer Ther*. 2008;7(3):521–529.
11. Iida J, Dorchak J, Lehman JR, et al. FH535 inhibited migration and growth of breast cancer cells. *PLoS One*. 2012;7(9):e44418.
12. Ren J, Wang R, Song H, Huang G, Chen L. Secreted frizzled related protein 1 modulates taxane resistance of human lung adenocarcinoma. *Mol Med*. 2014;20:164–178.
13. Hannigan G, Troussard AA, Dedhar S. Integrin-linked kinase: a cancer therapeutic target unique among its ILK. *Nat Rev Cancer*. 2005; 5(1):51–63.
14. Legate KR, Montanez E, Kudlacek O, Fassler R. ILK, PINCH and parvin: the tIPP of integrin signalling. *Nat Rev Mol Cell Biol*. 2006;7(1): 20–31.
15. Palacios F, Price L, Schweitzer J, Collard JG, D'Souza-Schorey C. An essential role for ARF6-regulated membrane traffic in adherens junction turnover and epithelial cell migration. *EMBO J*. 2001;20(17): 4973–4986.
16. Pece S, Gutkind JS. E-cadherin and Hakai: signalling, remodeling or destruction? *Nat Cell Biol*. 2002;4(4):E72–E74.
17. D'Souza-Schorey C. Disassembling adherens junctions: breaking up is hard to do. *Trends Cell Biol*. 2005;15(1):19–26.
18. Tsukita S, Furuse M, Itoh M. Multifunctional strands in tight junctions. *Nat Rev Mol Cell Biol*. 2001;2(4):285–293.
19. Cheng CY, Mruk DD. Cell junction dynamics in the testis: sertoli-germ cell interactions and male contraceptive development. *Physiol Rev*. 2002;82(4):825–874.
20. Matter K, Balda MS. Signalling to and from tight junctions. *Nat Rev Mol Cell Biol*. 2003;4(3):225–236.
21. Balda MS, Matter K. Epithelial cell adhesion and the regulation of gene expression. *Trends Cell Biol*. 2003;13(6):310–318.
22. Bazzoni G, Dejana E. Endothelial cell-to-cell junctions: molecular organization and role in vascular homeostasis. *Physiol Rev*. 2004;84(3): 869–901.
23. Furuse M, Tsukita S. Claudins in occluding junctions of humans and flies. *Trends Cell Biol*. 2006;16(4):181–188.
24. Linder S. The matrix corroded: podosomes and invadopodia in extracellular matrix degradation. *Trends Cell Biol*. 2007;17(3): 107–117.
25. Chhabra ES, Higgs HN. The many faces of actin: matching assembly factors with cellular structures. *Nat Cell Biol*. 2007;9(10):1110–1121.
26. McEver RP, Zhu C. Rolling cell adhesion. *Annu Rev Cell Dev Biol*. 2010;26:363–396.
27. Parsons JT, Horwitz AR, Schwartz MA. Cell adhesion: integrating cytoskeletal dynamics and cellular tension. *Nat Rev Mol Cell Biol*. 2010; 11(9):633–643.
28. Mullins RF, Skeie JM, Folk JC, et al. Evaluation of variants in the selectin genes in age-related macular degeneration. *BMC Med Genet*. 2011;12:58.
29. Ciriza J, Garcia-Ojeda ME. Expression of migration-related genes is progressively upregulated in murine lineage-Sca-1+c-Kit+ population from the fetal to adult stages of development. *Stem Cell Res Ther*. 2010; 1(2):14.
30. Kaartinen V, Voncken JW, Shuler C, et al. Abnormal lung development and cleft palate in mice lacking TGF-beta 3 indicates defects of epithelial-mesenchymal interaction. *Nat Genet*. 1995;11(4):415–421.
31. Timmerman LA, Grego-Bessa J, Raya A, et al. Notch promotes epithelial-mesenchymal transition during cardiac development and oncogenic transformation. *Genes Dev*. 2004;18(1):99–115.
32. Moreno-Bueno G, Cubillo E, Sarrió D, et al. Genetic profiling of epithelial cells expressing E-cadherin repressors reveals a distinct role for snail, slug, and E47 factors in epithelial-mesenchymal transition. *Cancer Res*. 2006;66(19):9543–9556.
33. Yang J, Weinberg RA. Epithelial-mesenchymal transition: at the crossroads of development and tumor metastasis. *Dev Cell*. 2008;14(6): 818–829.
34. Hoffman AE, Zheng T, Ba Y, et al. Phenotypic effects of the circadian gene cryptochrome 2 on cancer-related pathways. *BMC Cancer*. 2010;10:110.
35. Tetsu O, McCormick F. Beta-catenin regulates expression of cyclin D1 in colon carcinoma cells. *Nature*. 1999;398(6726):422–426.
36. Fearon ER. PARsing the phrase “all in for axin” – Wnt pathway targets in cancer. *Cancer Cell*. 2009;16(5):366–368.
37. White BD, Chien AJ, Dawson DW. Dysregulation of Wnt/beta-catenin signaling in gastrointestinal cancers. *Gastroenterology*. 2012;142(2): 219–232.
38. MacDonald BT, Tamai K, He X. Wnt/beta-catenin signaling: components, mechanisms, and diseases. *Dev Cell*. 2009;17(1):9–26.
39. Di Cristofano A, Pandolfi PP. The multiple roles of PTEN in tumor suppression. *Cell*. 2000;100(4):387–390.
40. Waite KA, Eng C. Protean PTEN: form and function. *Am J Hum Genet*. 2002;70(4):829–844.
41. Chalhoub N, Baker SJ. PTEN and the PI3-kinase pathway in cancer. *Annu Rev Pathol*. 2009;4:127–150.
42. Wang H, Chen P, Liu XX, et al. Prognostic impact of gastrointestinal bleeding and expression of PTEN and Ki-67 on primary gastrointestinal stromal tumors. *World J Surg Oncol*. 2014;12:89.
43. Tang H, Yao L, Tao X, et al. miR-9 functions as a tumor suppressor in ovarian serous carcinoma by targeting TLN1. *Int J Mol Med*. 2013; 32(2):381–388.
44. Sakamoto S, McCann RO, Dhir R, Kyprianou N. Talin1 promotes tumor invasion and metastasis via focal adhesion signaling and anoikis resistance. *Cancer Res*. 2010;70(5):1885–1895.
45. Sommers CL, Byers SW, Thompson EW, Torri JA, Gelmann EP. Differentiation state and invasiveness of human breast cancer cell lines. *Breast Cancer Res Treat*. 1994;31(2–3):325–335.
46. Zhu H, Lu J, Wang X, et al. Upregulated ZO-1 correlates with favorable survival of gastrointestinal stromal tumor. *Med Oncol*. 2013;30(3): 631.
47. Doi Y, Yashiro M, Yamada N, Amano R, Noda S, Hirakawa K. VEGF-A/VEGFR-2 signaling plays an important role for the motility of pancreas cancer cells. *Ann Surg Oncol*. 2012;19(8):2733–2743.
48. Walsh N, Clynes M, Crown J, O'Donovan N. Alterations in integrin expression modulates invasion of pancreatic cancer cells. *J Exp Clin Cancer Res*. 2009;28:140.
49. Sena P, Mariani F, Marzona L, et al. Matrix metalloproteinases 15 and 19 are stromal regulators of colorectal cancer development from the early stages. *Int J Oncol*. 2012;41(1):260–266.
50. Wu Y, Zhou BP. Snail: more than EMT. *Cell Adh Migr*. 2010;4(2): 199–203.
51. Fan F, Samuel S, Evans KW, et al. Overexpression of snail induces epithelial-mesenchymal transition and a cancer stem cell-like phenotype in human colorectal cancer cells. *Cancer Med*. 2012;1(1):5–16.

52. Hotz B, Arndt M, Dullat S, Bhargava S, Buhr HJ, Hotz HG. Epithelial to mesenchymal transition: expression of the regulators snail, slug, and twist in pancreatic cancer. *Clin Cancer Res.* 2007;13(16):4769–4776.
53. von Burstin J, Eser S, Paul MC, et al. E-cadherin regulates metastasis of pancreatic cancer in vivo and is suppressed by a SNAIL/HDAC1/HDAC2 repressor complex. *Gastroenterology.* 2009;137(1):e361–e365.
54. Shin NR, Jeong EH, Choi CI, et al. Overexpression of snail is associated with lymph node metastasis and poor prognosis in patients with gastric cancer. *BMC Cancer.* 2012;12:521.
55. Kuo KT, Chou TY, Hsu HS, Chen WL, Wang LS. Prognostic significance of NBS1 and snail expression in esophageal squamous cell carcinoma. *Ann Surg Oncol.* 2012;19(suppl 3):S549–S557.
56. van Nes JG, de Kruijf EM, Putter H, et al. Co-expression of SNAIL and TWIST determines prognosis in estrogen receptor-positive early breast cancer patients. *Breast Cancer Res Treat.* 2012;133(1):49–59.
57. Wu Y, Zhou BP. New insights of epithelial-mesenchymal transition in cancer metastasis. *Chin J Biochem Biophys.* 2008;40(7):643–650.
58. Friess H, Yamanaka Y, Büchler M, et al. Enhanced expression of transforming growth factor beta isoforms in pancreatic cancer correlates with decreased survival. *Gastroenterology.* 1993;105(6):1846–1856.
59. Rowland-Goldsmith MA, Maruyama H, Kusama T, Ralli S, Korc M. Soluble type II transforming growth factor-beta (TGF-beta) receptor inhibits TGF-beta signaling in COLO-357 pancreatic cancer cells in vitro and attenuates tumor formation. *Clin Cancer Res.* 2001;7(9):2931–2940.
60. Melisi D, Ishiyama S, Scialabba GM, et al. LY2109761, a novel transforming growth factor beta receptor type I and type II dual inhibitor, as a therapeutic approach to suppressing pancreatic cancer metastasis. *Mol Cancer Ther.* 2008;7(4):829–840.
61. Misra S, Sharma S, Agarwal A, et al. Cell cycle-dependent regulation of the bi-directional overlapping promoter of human BRCA2/ZAR2 genes in breast cancer cells. *Mol Cancer.* 2010;9:50.
62. Lu H, Yue J, Meng X, Nickoloff JA, Shen Z. BCCIP regulates homologous recombination by distinct domains and suppresses spontaneous DNA damage. *Nucleic Acids Res.* 2007;35(21):7160–7170.
63. Liu X, Cao L, Ni J, et al. Differential BCCIP gene expression in primary human ovarian cancer, renal cell carcinoma and colorectal cancer tissues. *Int J Oncol.* 2013;43(6):1925–1934.
64. Huang YY, Dai L, Gaines D, et al. BCCIP suppresses tumor initiation but is required for tumor progression. *Cancer Res.* 2013;73(23):7122–7133.
65. Cui X, Yu L, Wang Y, et al. The relationship between cyclin G1 and survival in patients treated surgically for HCC. *Hepatogastroenterology.* 2013;60(121):153–159.
66. Wen W, Ding J, Sun W, et al. Cyclin G1-mediated epithelial-mesenchymal transition via phosphoinositide 3-kinase/Akt signaling facilitates liver cancer progression. *Hepatology.* 2012;55(6):1787–1798.
67. Li J, Muscarella P, Joo SH, et al. Dissection of CDK4-binding and transactivation activities of p34(SEI-1) and comparison between functions of p34(SEI-1) and p16(INK4A). *Biochemistry.* 2005;44(40):13246–13256.
68. Tang DJ, Hu L, Xie D, et al. Oncogenic transformation by SEI-1 is associated with chromosomal instability. *Cancer Res.* 2005;65(15):6504–6508.
69. van Dekken H, Alers JC, Riegman PH, Rosenberg C, Tilanus HW, Vissers K. Molecular cytogenetic evaluation of gastric cardia adenocarcinoma and precursor lesions. *Am J Pathol.* 2001;158(6):1961–1967.
70. Tang TC, Sham JS, Xie D, et al. Identification of a candidate oncogene SEI-1 within a minimal amplified region at 19q13.1 in ovarian cancer cell lines. *Cancer Res.* 2002;62(24):7157–7161.
71. Hsu SI, Yang CM, Sim KG, Hentschel DM, O'Leary E, Bonventre JV. TRIP-Br: a novel family of PHD zinc finger- and bromodomain-interacting proteins that regulate the transcriptional activity of E2F-1/DP-1. *EMBO J.* 2001;20(9):2273–2285.
72. Sugimoto M, Nakamura T, Ohtani N, et al. Regulation of CDK4 activity by a novel CDK4-binding protein, p34(SEI-1). *Genes Dev.* 1999;13(22):3027–3033.
73. Hong SW, Kim CJ, Park WS, et al. p34SEI-1 inhibits apoptosis through the stabilization of the X-linked inhibitor of apoptosis protein: p34SEI-1 as a novel target for anti-breast cancer strategies. *Cancer Res.* 2009;69(3):741–746.

OncoTargets and Therapy

Publish your work in this journal

OncoTargets and Therapy is an international, peer-reviewed, open access journal focusing on the pathological basis of all cancers, potential targets for therapy and treatment protocols employed to improve the management of cancer patients. The journal also focuses on the impact of management programs and new therapeutic agents and protocols on

Submit your manuscript here: <http://www.dovepress.com/oncotargets-and-therapy-journal>

patient perspectives such as quality of life, adherence and satisfaction. The manuscript management system is completely online and includes a very quick and fair peer-review system, which is all easy to use. Visit <http://www.dovepress.com/testimonials.php> to read real quotes from published authors.

Dovepress